# Characterization and Modelling of the Multiaxial Fatigue Response of Glass Fibre Reinforced Composite Materials

Glud, Jens Ammitzbøll

*DOI (link to publication from Publisher):*
10.5278/vbn.phd.eng.00009

*Publication date:*
2017

*Document Version*
Publisher's PDF, also known as Version of record

# CHARACTERIZATION AND MODELLING OF THE MULTIAXIAL FATIGUE RESPONSE OF GLASS FIBRE REINFORCED COMPOSITE MATERIALS

**BY**
**JENS GLUD**

DISSERTATION SUBMITTED 2017

AALBORG UNIVERSITY
DENMARK

# CHARACTERIZATION AND MODELLING OF THE MULTIAXIAL FATIGUE RESPONSE OF GLASS FIBRE REINFORCED COMPOSITE MATERIALS

by

Jens Glud

AALBORG UNIVERSITY
DENMARK

Dissertation submitted

.

| | |
|---|---|
| Thesis submitted: | 08-05-2017 |
| Principal Ph.D. supervisor: | Associate Prof. Lars Christian Terndrup Overgaard, Aalborg University |
| Ph.D. co-supervisor: | Prof. Ole Thybo Thomsen, University of Southampton,<br>Prof. Janice Marie Dulieu-Barton, University of Southampton |
| Ph.D. committee: | Prof. Stephen Ogin, University of Surrey<br>Assoc. Prof. Christian Berggreen, Technical University of Denmark<br>Assoc. Prof. Jan Schjødt-Thomsen, Aalborg University |
| Ph.D. Series: | Faculty of Engineering and Science, Aalborg University |

ISSN (online): 2446-1636
ISBN (online): 978-87-7112-961-8

Published by:
Aalborg University Press
Skjernvej 4A, 2nd floor
DK – 9220 Aalborg Ø
Phone: +45 99407140
aauf@forlag.aau.dk
forlag.aau.dk



Printed in Denmark by Rosendahls, 2017

# PREFACE

This Ph.D. thesis was submitted to the Faculty of Engineering and Science at Aalborg University. The Ph.D. thesis presents the research carried out during the course of a Ph.D. project at the Department for Mechanical and Manufacturing Engineering at Aalborg University from September 2013 to September 2016. The project has received sponsorship from Innovation Fund Denmark through the Danish Centre for Composite Structures and Materials for Wind Turbines (DCCSM). The support received is gratefully acknowledged.

The central part of the research conducted during the project period appears in four papers, two papers have been published in international scientific journals with peer review, whilst the two others were both undergoing review for possible publication in international journals at the time of printing of this thesis. This thesis is structured as an extended summary of these four papers to frame them in the context of the Ph.D. project. This thesis includes (1) a general summary of and the motivation for the research carried out and documented in the four papers, (2) conclusions and (3) a discussion of future work. All the papers can be found in the appendix chapters of this Ph.D. thesis.

The project has been supervised by Associate Professor Lars Christian Terndrup Overgaard, Department of Mechanical and Manufacturing Engineering, Aalborg University, Professor Ole Thybo Thomsen, affiliated with both the Department of Mechanical and Manufacturing Engineering (AAU) and the Faculty of Engineering and the Environment, University of Southampton and finally Professor Janice Dulieu-Barton, from the Faculty of Engineering and the Environment, University of Southampton. I would like to extend my sincere gratitude to all of my supervisors for the excellent guidance and support I have received throughout the entire project period.

Parts of the research in this Ph.D. project have been carried out during international placements. I have spent four months at the University of Southampton, United Kingdom, in the research group of Engineering Materials under the supervision of Professor Janice Dulieu-Barton. Another four months were spent at the Department of Management and Engineering at the University of Padova, Italy, under the supervision of Professor Marino Quaresimin and Assistant Professor Paolo Carraro. I am very grateful for the guidance, support and fruitful discussions during these external collaborations.

My family and especially my wonderful girlfriend Marie-Louise have always supported me during the project, for which I am very thankful.

Jens Glud, May 2017

# ENGLISH SUMMARY

The main purpose of this Ph.D. project was to develop a physically based fatigue model for intralaminar damage in glass-fibre reinforced polymer (GFRP) laminates when subjected to multiaxial fatigue loading. An automated in-situ measurement and post-processing method named Automatic Crack Counting (ACC) was developed to monitor and analyse the layer-wise off-axis crack evolution in Multi-Directional (MD) GFRP laminates. The method uses transilluminated white light imaging and a digital camera to capture images of the crack evolution. An algorithm was developed to automatically analyse these images. The outcome of this work is a methodology that enables automatic layer-wise quantification of the off-axis crack damage state, i.e. the number, length and location of initiated cracks, measured throughout the fatigue test in a consistent and reliable manner (Paper #1).

The ACC method was complemented with in-situ measurements of the material strain using lock-in Digital Image Correlation (DIC) and an extensometer to measure the change in stiffness of a series of tested GFRP laminates. The full experimental setup was used for monitoring fatigue tests of GFRP plies embedded in a multidirectional laminate such that stable damage evolution was achieved. Opposite to earlier observations with unstable propagation at the weakest material point with a single crack growth, it was demonstrated how the high-temporal resolution of ACC could be used to study the damage evolution with a level of detail never before achieved. It was found that the number of cycles to crack initiation of isolated cracks and the crack growth rate for a constant energy release rate exhibited a large scatter for the tested GFRP material system. The Weibull distribution was shown to accurately model the stochastic nature of crack initiation and growth. The crack density was found to be a suitable damage measure for history dependent effects in the form of variable amplitude loading. It was further established that the compression-tension loading was less damaging than tension-tension loading for identical load amplitude. Using the measured change in compliance from the lock-in DIC and extensometer measurements, the micro-mechanical stiffness degradation model called GLOB-LOC was found to slightly under-predict the stiffness change of the damaged laminate when using ACC to measure the crack densities required as input for the GLOB-LOC model (Paper #2).

The off-axis damage evolution in GFRP laminates is a multi-scale and hierarchical process involving several length scales. The process consists of off-axis crack initiation at the scale of the inter-fibre distance and off-axis propagation at the scale of the overall structure. Efficient multi-scale stress analysis tools are needed to model such a complicated process. In addition, reliable models, that describe the damage evolution rate as function of the local stress state obtained from the multiscale stress analysis tools are needed to predict the full damage evolution. In literature, it was found that the experimentally observed crack propagation rate for

off-axis cracks in MD laminates subjected to multiaxial-loading depend on the local mode-mixity of the off-axis crack front. However, there have not been published any physically based models suitable for predicting the influence of the local mode-mixity on the crack propagation rate in open literature. Therefore, a physically based crack propagation model has been developed along with a multi-scale approach used to produce the model predictions in a computationally efficient manner. The development of this model was carried out in collaboration with the research group of Professor Marino Quaresimin at the University of Padova, Italy. The model requires experimental data from two different mixed-mode loading conditions in order to derive two Paris' Law master curves for a given composite system. Based on these master curves, the model is capable of predicting the crack growth rate for the entire local mode-mixity range as long as friction does not play an important role. The model has been shown to work for off-axis cracks in GFRP tubes and delaminations in both GFRP and carbon-fibre reinforced polymer laminates (Paper #3).

The ACC method from Paper #1, the conclusions from Paper #2 and the modelling of off-axis crack propagation presented in Paper #3 enabled the development of a physically based multiaxial fatigue model framework (Paper #4). The main constituents used in the developed multiaxial fatigue model are the GLOB-LOC model, a physically based multiaxial initiation criterion and the crack propagation model from (Paper #3). The GLOB-LOC model was extended to predict the variations in stress field between interacting off-axis cracks, in order to apply the extended GLOB-LOC model for a complete range of crack densities in the evaluation of multiaxial initiation and mixed mode propagation. The new physically based model framework has been found to provide good predictions for the crack density evolution in thick off-axis GFRP layers subjected to multiaxial fatigue.

# DANSK RESUME

Det overordnede mål for dette Ph.D. projekt har været at udvikle en fysisk baseret udmattelsesmodel til modellering af skaderne i de enkelte lag af glasfiberforstærket polymerlaminater (GFRP), når disse udsættes for multi-aksielle udmattelseslaster. En automatiseret målemetode kaldt Automatic Crack Counting (ACC) er blevet udviklet til formålet, således at revner i hvert enkelt lag kan detekteres og monitoreres. Målemetoden anvender gennemlysning af prøveemner med hvidt lys og et digitalt kamera til at tage billeder af lyset. Til at analysere de optagede billeder er der blevet udviklet en numerisk algoritme. Denne algoritme er i stand til automatisk at kvantificere revnevækst i de enkelte GFRP lag, hvilket indebærer en konsistent og pålidelig opmåling af antallet af revner, deres længde og placering igennem hele tidsforløbet af udmattelsestestene (artikel #1).

ACC forsøgsopstillingen er blevet udvidet med tøjningsmålinger ved hjælp af Lock-In Digital Image Correlation (DIC) og ekstensometer for at fastlægge materialets stivhedsdegradering under udmattelsestestene. Denne forsøgsopstilling blev anvendt til at analysere udmattelsesskader i de individuelle GFRP lag i et laminat bestående af flere GFRP lag, som var orienteret forskelligt for at skabe en stabil revnevækst. I modsætning til tidligere observationer af ustabil revnevækst ved det svageste materialepunkt, blev det demonstreret hvordan den høje tidsopløsning ved brug af ACC kunne bruges til at studere skadesudviklingen med en detaljegrad som ikke er set tidligere. Der blev fundet en stor variation i antallet af belastninger påkrævet for at initiere nye revner, samt hvor hurtigt allerede eksisterende revner vokser. Det er blevet vist at Weibull fordelingen præcist modellerer denne variation. Revnedensiteten er blevet fastlagt til at være en anvendelig skadesparameter, når historie afhængige lastspektre skal modelleres for GFRP materiale. Tryk-træk udmattelseslaster er mindre skadende end træk-træk laster, når lastamplituden forbliver uændret. Den målte stivhedsdegradering er blevet sammenholdt med model resultater fra den mikro-mekaniske stivhedsdegraderingsmodel kaldet GLOB-LOC. Revnedensitetsmålinger fra ACC blev brugt som input til GLOB-LOC, og det blev observeret at GLOB-LOC underprædikterer stivheden af de skadede laminater (artikel #2).

Revneudvikling i GFRP laminater er en multiskala og hierarkisk proces som involverer flere forskellige længdeskalaer. Processen består af revneinitiering som skyldes udviklingen af mikrorevner i matricematerialet mellem fibre samt revnevækst som kan strække sig til hele strukturen. Effektive værktøjer til multiskala spændingsanalyse er derfor nødvendige for at modellere en så kompliceret skadesproces. Ydermere, er pålidelige modeller, der beskriver skadesudviklingen som funktion af de lokale spændinger bestemt ved multiskala analyse, nødvendige for at kunne beskrive den fulde skadesudvikling. I den offentligt tilgængelige litteratur er det almen kendt at revnevækstshastigheden i

GFRP afhænger af revnefrontens lokale lastpåvirkning. Ingen fysisk baserede modeller til at beskrive indflydelsen af lokal lastpåvirkning på revnevækst hastigheden i GFRP laminater var tilgængelige i litteraturen. Derfor blev en sådan fysisk model samt en multiskala tilgang til at evaluere modellen ved brug af begrænsede computer ressourcer udviklet. Udviklingen af denne model blev foretaget i samarbejde med Marino Quaresimins forskningsgruppe ved Universitetet i Padova, Italien. Modellen kræver eksperimentelle data fra to forskellige måder at laste revnefronten på, således to styrende regressionskurver af Paris' Lov kan blive udledt. Baseret på disse regressionskurver er modellen i stand til at forudsige revnevækstshastigheden for hele spændet af mulige revnefrontslaster, så længe friktion ikke spiller en væsentlig rolle. Det er blevet vist, hvorledes modellen virker for både revner i de enkelte GFRP lag i rørgeometrier men også, hvorledes modellen virker for delamineringer i GFRP- og kulfiberforstærket polymer laminater (artikel #3).

ACC metoden fra artikel #1, konklusionerne draget i artikel #2 og modellen til at forudsige hastigheden af revnevækst fra artikel #3 gjorde det muligt at udvikle den fysisk baserede udmattelsesmodel som er præsenteret i artikel #4. Hovedbestanddelene i denne model er GLOB-LOC modellen kombineret med en multi-aksiel initieringsmodel fra litteraturen og revnevækst modellen fra artikel #3. GLOB-LOC blev udvidet således at modellen kunne beskrive de variationer som opstår i spændingsfeltet, når revner i GFRP lagene begynder at interagere. Dette var nødvendigt for det valgte multi-aksielle initieringskriterie og den udviklede revnevækst model kunne evalueres. Det er blevet demonstreret, hvorledes den fysisk baserede udmattelsesmodel kan forudsige udviklingen af revnedensiteten i tykke GFRP lag, når disse udsættes for multi-aksielle udmattelseslaster.

# PUBLICATIONS

Parts of the research conducted in this project have been published.

### Papers published in international journals with peer review:

- **(Paper #1)**: Glud JA, Dulieu-Barton JM, Thomsen OT, Overgaard LCT. Automated counting of off-axis tunnelling cracks using digital image processing. Compos Sci Technol 2016;125:80–9. doi:10.1016/j.compscitech.2016.01.019.
- **(Paper #2)**: Glud JA, Dulieu-Barton JM, Thomsen OT, Overgaard LCT. Fatigue damage evolution in GFRP laminates with constrained off-axis plies. Compos Part A Appl Sci Manuf 2017;95:359–69. doi:10.1016/j.compositesa.2017.02.005.

### Papers submitted to international journals with peer review:

- **(Paper #3)**: Glud JA, Carraro PA, Quaresimin M, Dulieu-Barton JM, Thomsen OT, Overgaard LCT. A physically based model for off-axis fatigue crack propagation in FRP composites. Submitted;Under Review.

### Papers accepted by international journals with peer review:

- **(Paper #4)**: Glud JA, Dulieu-Barton JM, Thomsen OT, Overgaard LCT. A stochastic multiaxial fatigue model for off-axis cracking in FRP laminates. Accepted; International Journal of Fatigue.

### Papers in international conferences with review:

- Glud JA, Overgaard LCT, Dulieu-Barton JM, Thomsen OT. Intralaminar fatigue characterization of GFRP laminate using lock-in DIC and TSA for use in micro-mechanics based multiaxial fatigue model. 7th Int. Conf. Compos. Test. Model Identif. (CompTest 2015), Getafe, Spain, 2015. (won best student oral presentation award)
- Glud JA, Dulieu-Barton JM, Thomsen OT, Overgaard LCT. Micro-mechanical multiaxial fatigue model for crack density evolution and stiffness degradation. 20th Int. Conf. Compos. Mater. (ICCM20), Copenhagen, Denmark, 2015, p. 1204–1.
- Glud JA, Dulieu-Barton JM, Thomsen OT, Overgaard LCT. A new white light imaging approach for intralaminar fatigue characterisation of GFRP. 10th Int. Conf. Exp. Mech., (ICEM-10), Edinburgh, UK, 2015. (won Young Stress Analysts award)
- Glud JA, Dulieu-Barton JM, Thomsen OT, Overgaard LCT. Data rich multiaxial fatigue characterisation of off-axis layers in GFRP laminates. BSSM's First Postgrad. Exp. Mech. Conf., Southampton, UK, 2015.
- Glud JA, Dulieu-Barton JM, Thomsen OT, Overgaard LCT. Efficient micro-mechanical multiaxial fatigue testing and modelling for GFRP

laminates. Eur. Conf. Compos. Mater., (ECCM-16), Munich, Germany, 2016.

# TABLE OF CONTENTS

# CHAPTER 1. BACKGROUND AND MOTIVATION

Glass fibre reinforced polymers (GFRP) were invented during the 1940's and when compared to e.g. steel this can be considered to be a relatively new type of material. It consists of glass fibres hold together by a matrix material made from polymers. A rapid growth in the use of GFRP materials has been observed since its invention and in 2014 95% of the world wide total production of FRP materials was GFRP [1]. GFRP laminates belong to a specific class of GFRP material where glass fabrics made from continuous fibres are stacked on top of each other and impregnated by a polymer resin to create a solid composite material. GFRP laminates are being used increasingly in structural components where the strength to weight ratio is important. Accurate models that can predict when the material fails are required to fully utilise the strength to weight ratio of GFRP laminates.

To predict failure of GFRP laminates a wide range of models has been proposed for quasi-static load cases. The world-wide-failure-exercise reviewed several of these models [2] and from this review it was pointed out that even the best performing models showed a poor predictive capability for several of the test cases.

Besides structural GFRP components susceptible to quasi-static failure, GFRP laminates are also being used increasingly in structural components subjected to fatigue loading. Examples of such components are modern wind turbine blades, which utilise large amounts of GFRP laminate materials. The gravitational, inertial and aerodynamic loads acting on a wind turbine blade are fatigue loads. Wind turbine blades have a service life of more than 20 years, and are therefore subjected to ultra-high cycle fatigue. The fatigue loading experienced by the GFRP laminates is multiaxial and causes strength and stiffness degradation, which leads to a finite lifetime of the blades. Modern wind turbine blades are so large that gravitational and inertial loads have started to dominate more than aerodynamic loads [3]. This means that wind turbine blades are now weight critical structures and therefore requires accurate fatigue models to utilise the material in the most efficient manner and hence save weight.

As for quasi-static loads, several models for predicting material failure of GFRP laminates subjected to fatigue loading have been proposed. The vast majority of these models are phenomenological and the most widely applied design methods used in e.g. the wind turbine industry makes use of these phenomenological models [4]. The phenomenological models currently proposed for GFRP laminates and the phenomenological models used by standards [4–6] are highly inspired by empirical models developed for metals. The models rely on stress versus life (S-N) diagrams as proposed by A. Wöhler for steel and account for the influence of mean stress

effects using constant life diagrams somewhat similar to the Goodman diagram approach developed by J. Goodman for steel. This appears to be a questionable approach considering the fact that the actual fatigue failure modes of the two types of materials are not similar. In steel, it is commonly recognised that the fatigue crack growth is explained by slip deformations of more than one slip plane which will cause crack extension and leave visible striations on crack surfaces [7,8]. When the crack reaches a critical length it becomes unstable resulting in a sudden catastrophic failure. Usually, the fatigue failure of GFRP laminates is not sudden as the material steadily degrades due to a series of subcritical failure modes. These failure modes and when they occur during the fatigue life of a GFRP laminate are schematically illustrated in Figure 1.

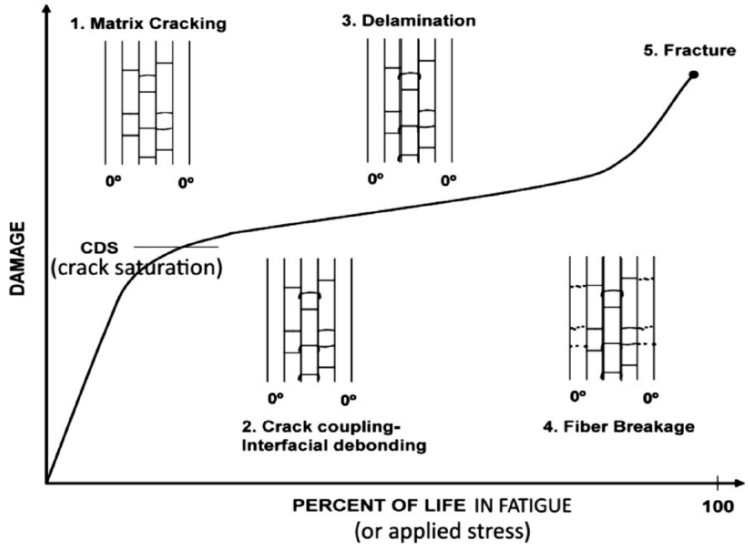


*Figure 1: Usual damage modes observed during fatigue loading of GFRP laminates* [9].

In GFRP laminates, the first damage mode usually takes the form of matrix cracking (also known as off-axis cracks or Inter Fibre Failure (IFF)) tunnelling through the laminate layers, followed by delamination and fibre breakage leading to ultimate structural failure. Thus, the fatigue damage process of GFRP is very different from the fatigue damage process in steel.

In a recent review of phenomenological fatigue models [10] for composite lamintes it was found that all reviewed models for several load cases provided overly conservative predictions and for several other load cases provided highly non-conservative predictions. Therefore, Quaresimin et al. [10] have questioned the general validity of the reviewed models and highlight the need for new and more

advanced models in order to use the materials in a more efficient manner. Quaresimin et al. [10] stress that research within the field of fatigue of laminated composites should move in the direction to improve the understanding of the underlying damage mechanisms, and further to include these damage mechanisms in future predictive models. The potential outcome of such an approach is envisaged to be generally applicable models, which would limit the need for experimental testing, provide enhanced information of the actual damage states within the material, and finally provide better lifetime predictions. All of these outcomes may help the composites industry in creating lighter, cheaper and more efficient composite products.

Fatigue models for composite laminates, which incorporate actual damage mechanisms, are still in their infant stage [11], since they are limited to simple laminate configurations and restricted to simple fatigue load cases. The reason why this branch of fatigue models are still in their infant stage despite their appealing envisaged outcome could be explained by the limited amount of experimental studies of actual damage mechanisms [12] and the fact that fatigue damage is a complicated multi-scale and hierarchical process occurring at several different length scales [13]. This, underpins the need for advancing both the experimental and the modelling research fields in order to reach the ultimate goal of having models capable of providing safe and reliable fatigue life predictions for composite laminates.

## 1.1. RESEARCH OBJECTIVES

The overall objective of the Ph.D. project is to develop an improved understanding of failure mechanisms in multi-directional GFRP laminates and to propose a fatigue life prediction model for GFRP laminates, which models the actual fatigue damage evolution process. This includes the following sub-goals of the research:

- A new method to characterise multiaxial fatigue in GFRP laminates.
- Experimental investigation of off-axis cracks in GFRP laminates under multiaxial fatigue loading.
- Physically based modelling of off-axis cracks in GFRP laminates and its influence on the in-plane elastic properties of the damaged laminate.

The anticipated outcome is a multiaxial fatigue model capable of describing the actual off-axis crack damage mechanisms in GFRP laminates and an efficient test campaign strategy to fatigue characterise a GFRP material.

The following chapters summarise the research conducted during this Ph.D. project and the conclusions drawn based on the research.

## 1.2. NOVELTY

The research conducted during this Ph.D. project has provided several novel contributions within the field of multiaxial fatigue testing and modelling of fatigue damage in multidirectional GFRP laminates. The novelties are described in detail in the four appended papers and can be summarised as follows:

- A novel in-situ experimental technique named Automatic Crack Counting (ACC) used to quantify fatigue damage in off-axis plies has been proposed. The method employs transilluminated white light imaging and digital image processing to automatically quantify the damage state. The in-situ and automatic nature of the method results in a high temporal resolution of the damage development in the tested laminates. (Paper #1)

- The fatigue damage evolution in GFRP off-axis plies has been studied in detail using the novel experimental technique, ACC (Paper #2). The tested off-axis plies have been subjected to different fatigue loading conditions taking into account both R-ratio effects and variable amplitude loading. Several new conclusions about how fatigue damage develops in multidirectional laminates have been drawn. The crack density was found to be a suitable damage measure for a low-high sequence of variable amplitude block loading. T-T loading results in a higher crack density than is the case for C-T loading for the same load amplitude. The Weibull distribution effectively models the stochastic nature of off-axis crack initiation and growth and the shape parameter of the Weibull distribution is independent of stress level and ply thickness. Furthermore, by using ACC it has been shown how to efficiently derive material parameters, which describe the off-axis crack damage evolution process.

- A physically based multi-scale model for modelling the influence of mixed-mode loading on the off-axis crack propagation rate under fatigue has been proposed (Paper #3). The local stress state in front of off-axis cracks was found to influence the observed microscopic damage modes responsible for crack propagation. Equivalent energy release rates based on the stress state associated with each of the observed damage modes were proposed. These equivalent energy release rates were found to be applicable for establishing two Paris' Law master curves, which can be used to describe the crack growth rate under different mixed-mode loading conditions.

- A new stochastic multi-scale fatigue model for modelling the off-axis crack evolution in multi-directional laminates has been developed (Paper #4).

The model is based on the GLOB-LOC [14] damage modelling framework, which in this project has been extended, so the multi-scale stress state of interacting cracks in the damaged plies can be accounted for. The model only requires two different laminate configurations to be tested in fatigue to calibrate the material parameters.

## 1.3. STRUCTURE OF THESIS

This Ph.D. thesis is based on four scientific papers, where Paper #1 and Paper #2 have been published in peer reviewed scientific journals and Paper #3 and Paper #4 have been submitted to peer reviewed scientific journals. The following chapters of this thesis present an extended summary of the research conducted and describes how the four papers are connected. The four papers are appended as annexes.

The extended summary is structured as follows:

- Chapter 1: Background and motivation for the project along with novelty claims and research objectives
- Chapter 2: Summary of Paper #1, where a novel experimental method to quantify the fatigue damage evolution in GFRP laminates is presented
- Chapter 3: Summary of Paper #2, where the novel experimental method from Paper #1 was used to study the damage evolution in an MD laminate containing off-axis plies
- Chapter 4: Benchmark of a state-of-the-art off-axis damage model against experimental measurements (Paper #2) and extension of the same damage model to include additional stress analysis capabilities (Paper #4)
- Chapter 5: Summary of Paper #3, which describes the development of a multiscale model to predict the crack growth rate of off-axis cracks under mixed-mode fatigue loadings
- Chapter 6: Summary of Paper #4, where a multiaxial fatigue model used to predict the off-axis crack evolution in MD laminates is described
- Chapter 7: Summary of scientific contributions
- Chapter 8: Suggestions for future work

# CHAPTER 2. EXPERIMENTAL METHOD TO CHARACTERISE FATIGUE DAMAGE EVOLUTION (PAPER #1)

Many different types of intralaminar micro damage may evolve during the fatigue life of laminated composites. One of the most common damage modes is intralaminar matrix cracks in the laminate layers, which are through-the-thickness (tunnelling) cracks in the matrix and fibre debonds propagating along the fibres. These cracks are commonly called off-axis matrix cracks in the research community. It is particularly important to predict the off-axis crack damage mode, since these cracks promote other damage modes such as delamination and fibre breakage [15,16] and are linked directly to the stiffness degradation observed in composite laminates during fatigue loading [17–20]. However, widely accepted models for predicting the off-axis crack evolution under either quasi-static or fatigue loading are yet to be proposed. The third world-wide failure exercise [21] focuses on the ability of currently existing models to predict off-axis crack evolution under quasi-static loading and the exercise has yet to be concluded. Furthermore, for the case of fatigue loading the need for such models is strongly emphasised in the recent review of phenomenological fatigue models in [10].

Even though off-axis cracks has received significant attention in literature, most experimental studies are limited with regard to their scope and coverage, and there is no general consensus on how the off-axis crack evolution should be measured, quantified and reported for laminated composites. Several different experimental techniques have been reported successful in detecting and measuring the off-axis crack evolution. These techniques include: thermoelastic stress analysis (TSA) [22], digital image correlation (DIC) [23], acoustic emission [24], X-ray [25], X-ray Computed Tomography (CT) [26], Ultrasonic C-scan [25], edge-examination [27] and transilluminated white light imaging (TWLI) [15,18–20,28]. Each technique has different capabilities when it comes to quantifying off-axis crack damage evolution. The different techniques are summarised in Table 1 according to a set of assessment criteria that are deemed important for the characterisation of off-axis crack evolution carried out in the present Ph.D. project.

| Method | Temporal Resolution | Automatic Quantification | Spatial resolution | Opaque Materials | Equipment Price |
|---|---|---|---|---|---|
| TSA | High | No | Medium (2.5D) | Yes | High |
| DIC | High | No | Medium (2.5D) | Yes | High |
| X-ray | Low | No | High (2.5D) | Yes | High |
| X-ray CT | Low | No | High (3D) | Yes | High |
| Ultrasonic C-scan | Low | No | Medium (2D) | Yes | High |
| Edge examination | Low | No | High (2D) | Yes | Low |
| TWLI | High | No | High (2.5D) | No | Low |
| Acoustic Emission | High | Yes | Low | Yes | Low |

*Table 1: Summary of capabilities of experimental techniques reported successful in measuring the off-axis crack damage evolution. (2.5D) means that some thickness information can be obtained if information about the layup is provided.*

An automatic quantification method with high temporal and spatial resolution was sought for in the context of the present research, so the off-axis damage evolution could be studied many times in a large volume of the test samples. X-ray, X-ray CT, Ultrasonic C-scan and edge examination require the fatigue test to be interrupted to conduct measurements and were therefore disregarded for the present research. TSA and DIC are in-situ surface measurement methods for obtaining the sum of maximum principal stresses and the component strain fields respectively. However, for some laminate configurations the stress and strain disturbances on the surface caused by subsurface cracks may be below the resolution of the TSA and DIC equipment, which will result in less robust crack detection. Acoustic emission is an in-situ and automated measurement method [24], but the damage mode connected with acoustic events has to be hypothesised or calibrated with other techniques. TWLI has a low price and a high temporal and spatial resolution but can only be used for transparent materials such as GFRP. Based upon the literature review of experimental techniques available for measuring off-axis cracks, TWLI was found to be the most favourable method for crack detection in the studied GFRP material system due to its transparency to white light. Consequently, TWLI was chosen as the basis for measuring the off-axis crack evolution in this research.

TWLI works by illuminating the material from one side and then acquiring images of the light transmitted through the material from the other side. The transmission of light is disrupted by the presence of off-axis cracks, which make them visible in the acquired images. Based on the review (Paper #1) of how TWLI has been used to detect and quantify off-axis cracks, it is clear that reported quantification processes, where information about the off-axis cracks has to be extracted from acquired

images, were manual and visual counting of cracks. The crack state generally consists of many cracks, which are unevenly distributed in the region of interest [9, 26]. Therefore, manual and visual counting is labour intensive and difficult to do in a consistent and reproducible manner. This limits the scope and size of studies and leads to a relatively poor temporal resolution of the crack state. Moreover, the material properties extracted from experimental tests and the drawn conclusion may not be valid, if the crack counting is not done in a consistent manner due to human mistakes in the counting process. It was therefore clear at the beginning of this Ph.D. project that there is a great need for developing an automated approach to quantify the crack state, so accurate and reproducible quantifications could be obtained in a fast, reliable and efficient manner.

## 2.1. TEST SETUP AND IMAGE ACQUISITION

Figure 2(a) shows an image and a sketch of the experimental setup used for fatigue testing of GFRP laminates and acquiring in-situ images of off-axis cracks using TWLI. The setup consists of a digital camera, which is placed on one side of the specimen. Both back and front side illumination are used in the test setup. LED lights are used as illumination sources to prevent the specimen from heating up. The front side illumination is used for motion compensation. Figure 2b illustrates the used specimen geometry along with important features on the specimen.

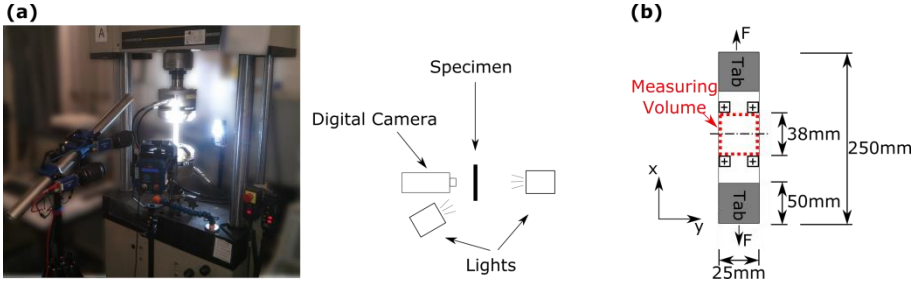


*Figure 2: (a) Experimental setup used for ACC. (b) Specimen, measuring volume and marker positions (Paper #1).*

Examples of acquired images of a 4.3mm thick laminate made from unidirectional stitched fibre mats with an areal weight of 600g/m$^2$ can be seen in Figure 3. The layup is $[0/-60/0/60]_s$ and the 0 plies are oriented along the x-axis in the figures. The image in Figure 3(a) is acquired before the fatigue test has been started and therefore there is no observable damage present in the image. An image acquired at a later instant during the fatigue test looks like Figure 3(b) and off-axis cracks are now readily visible. The stitching in the dry fibre mats has another refractive index than the glass fibres and the matrix material. This results in the texture seen in Figure 3. It

is clear that besides the complicated crack pattern seen in Figure 3(b), the stitching further complicates the problem of manual and visual counting of the developed off-axis cracks.

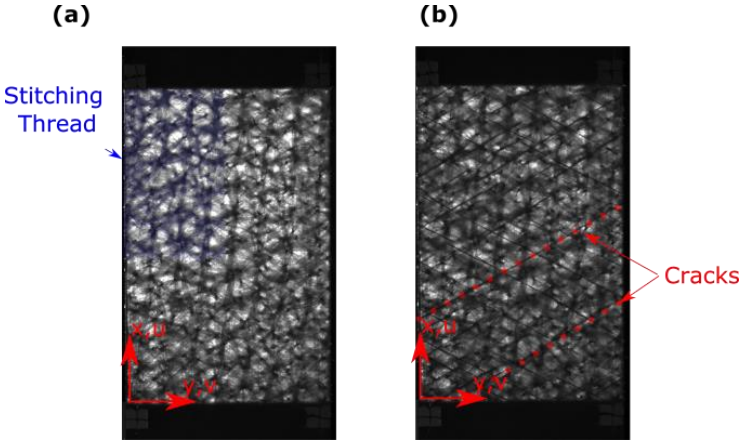


*Figure 3: (a) Measuring volume seen by the digital camera. Stitching threads in left upper corner is highlighted with blue. (b) In-situ observation of off-axis (Paper #1).*

## 2.2. THE ACC METHODOLOGY

The ACC method was developed to analyse images like those seen in Figure 3. The ACC method consists of three main image operations:

1. Image compensation
2. Image filtering
3. Crack counting

Off-axis cracks disrupt the light transmitted through the specimen. Therefore, the in-situ images ($I^i$) were compared with the image from the reference state ($I^r$) to distinguish original features in the image from new features which have originated due to damage development. However, such a comparison requires a means to correct for rigid body motion and deformation in the in-situ images and the purpose of the image compensation operation is to do those two corrections. The image compensation requires four markers attached on the front side of the specimen as seen in Figure 3. These markers may not change appearance and position on the specimen during the fatigue test. Therefore, it was decided to paint the markers on the specimen. Using 2D cross-correlation as described in (Paper #1) it is possible to

obtain the displacement for each marker, which may displace as sketched in Figure 4.

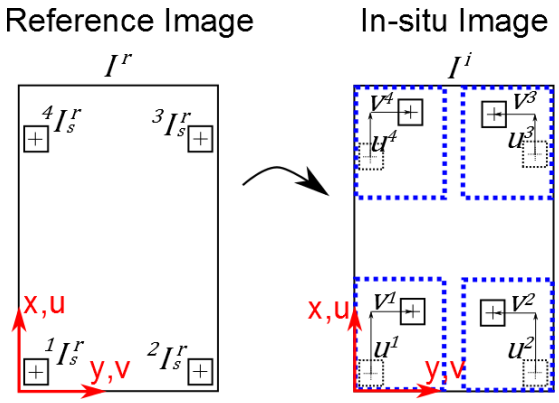


*Figure 4: Features defined in the reference image $I^r$ and afterwards found in the in-situ image $I^i$ (Paper #1).*

The displacement of each marker is used to compute the displacement fields *u(x, y)* and *v(x, y)*. The displacement fields are then used to compute the inverse linear 2D transformation matrix $(T)^{-1}$, which can be used to transform image $I^i$ to the position and reference state of image $I^r$ as $I^u(x,y) = (T)^{-1}I^i(x,y)$. $I^u$ is then compared to $I^r$ by a pixel wise normalisation given by $I^d(x,y) = I^u(x,y)/I^r(x,y)$. Figure 5(a) is an example of the normalized image $I^d$ obtained from the image compensation operation of the images in Figure 3.

The image compensation produces clear images of the developed off-axis cracks by removing features not related to damage. Further image filtering operations are required to study off-axis cracks in the different layers (orientations) independently from cracks in other layers. Gabor-filtering [30] was found to give consistent and reproducible results for this type of problem. To apply Gabor filtering four parameter settings are required as input to the algorithm. The meaning of the parameter settings and how to choose them are described in more details in (Paper #1). The resulting images when applying the Gabor filtering operation can be seen in Figure 5(b). From these images additional filtering operations are carried out to count the cracks. The images are thresholded using Otsu's method [31], followed by a thinning of lines using the method described in [32]. The resulting image consists of one pixel thick lines for each detected crack. The lengths of these lines are then measured by a heuristic counting procedure, which essentially determines the number of pixels belonging to each line and thereby the length of the crack. An example of counted cracks overlaid on $I^d$ from Figure 5(a) is seen in Figure 6.

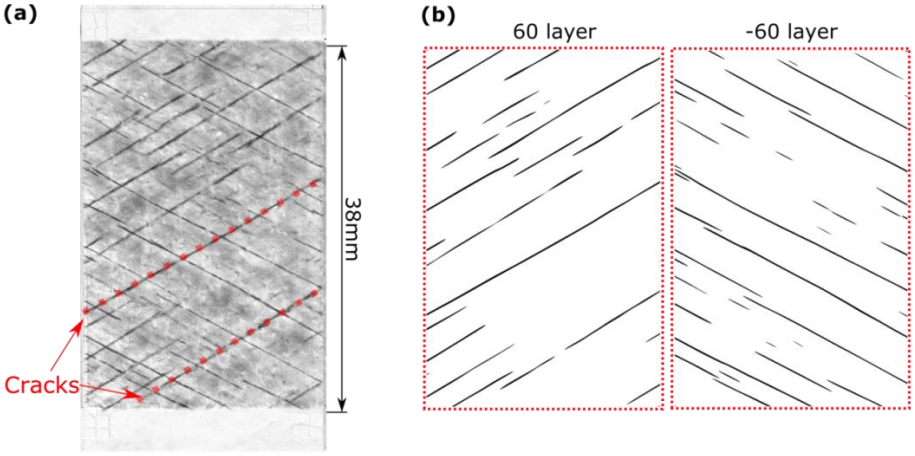


*Figure 5: a) Result of normalising the compensated in-situ image ($I^u$) with the reference image ($I^r$) to give the image of the damage ($I^d$). b) Result of Gabor filtering of image $I^d$ for each orientation of off-axis cracks (Paper #1).*

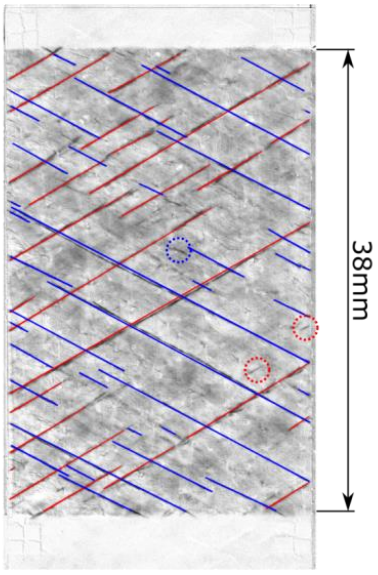


*Figure 6: Cracks counted by ACC in the image given in Figure 5a (blue is -60 degree layer, red is +60 degree layer) (Paper #1).*

It can be seen that virtually all the cracks are counted to their full length and have the proper orientation and location. The method of overlaying counted cracks on the

$I^d$ images has been used on several data sets to test the ACC method. Based on this it was concluded that ACC and its chain of main image operations work as intended with high accuracy, reliability and reproducibility.

## 2.3. VALIDATION

First, ACC was benchmarked by studying its accuracy when analysing synthetic images of off-axis cracks, where the crack density was known. Secondly, its accuracy was benchmarked against manual counting when ACC was used to process images obtained during fatigue tests. The crack density definition used for all studies is described in (Paper #1).

The purpose of one of the synthetic benchmarks carried out was to evaluate the accuracy of ACC when counting cracks in different layups. Figure 7(a) shows an example of a synthetic image with cracks in three different orientations and Figure 7(b) shows overlaid cracks as counted by ACC in the synthetic image.

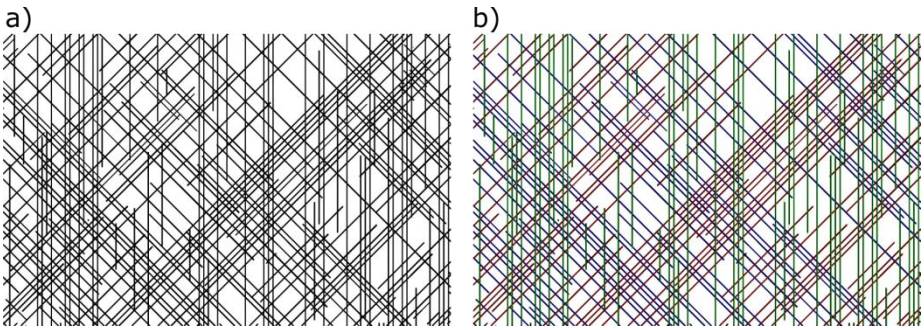


*Figure 7:a) Simulated cracks in [-45/45/90] laminate and b) cracks in simulated [-45/45/90] laminate counted by ACC (Paper #1).*

The relative error between the actual crack density in the synthetic image and the crack density as measured by ACC is plotted in Figure 8 for the five different simulated layups.

A maximum relative error in accuracy of less than 3% was found for this benchmark test. This accuracy was deemed sufficient to use ACC for counting off-axis cracks. The results from the benchmark of ACC against the manual counting can be seen in Figure 9.

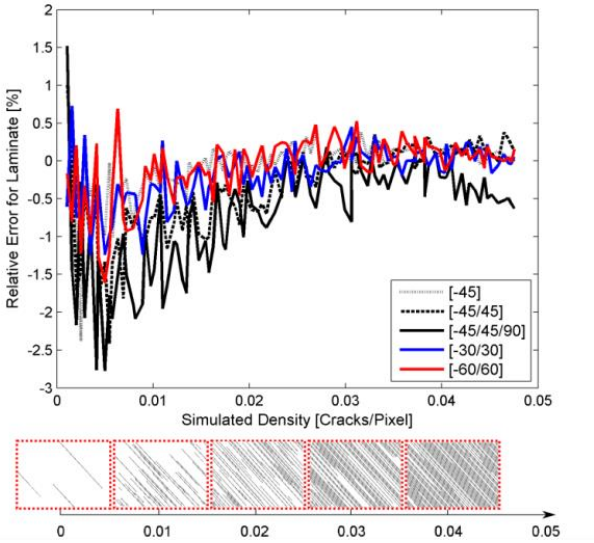


*Figure 8: Relative error of laminates between counted crack density and artificial crack density with examples of the artificial images for increasing crack density in one ply (Paper #1).*

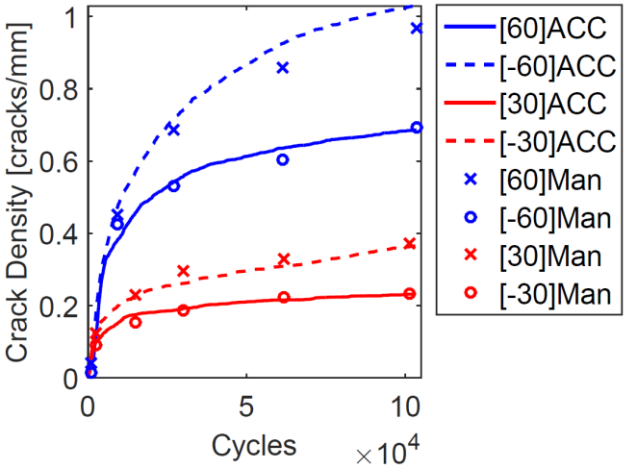


*Figure 9: Crack density as function of number of fatigue cycles measured for the different layers in a [0/-60/0/60]s and a [0/-30/0/30]s layup during the fatigue life using ACC and Manual counting (Man) (Paper #1).*

ACC and the manual counting agrees very well and the evolution curves as obtained by ACC is similar to evolution curves found in literature e.g. [18–20].

## 2.4. CONCLUSIONS

The research conducted in connection with the ACC algorithm led to the following conclusions:

- ACC makes it possible to acquire in-situ images of off-axis crack evolution without interrupting the fatigue test and subsequently analyse these images for off-axis cracks automatically (Paper #1).
- ACC is accurate in determining the length and location of off-axis cracks for several different types of multi-directional laminates (Paper #1).
- ACC counts the cracks in the entire image sequence without any user interaction after the initial steps of ACC have been completed. This includes choosing appropriate parameter settings and defining markers. Consequently, ACC represents a fast way of counting off-axis cracks (Paper #1).
- Due to the fact that ACC is a deterministic algorithm it provides reproducible results (Paper #1).
- To use ACC requires a very limited investment in measurement equipment, since it only requires a digital camera and two cold light sources, such as LED lights (Paper #1).

# CHAPTER 3. QUANTIFYING THE FATIGUE DAMAGE EVOLUTION IN GFRP LAMINATES (PAPER #2)

The increasing use of fibre reinforced polymer (FRP) laminates in the industry has led to several experimental campaigns aimed at quantifying the fatigue damage evolution in FRP laminates as function of the multiple factors (e.g. number of load reversals, magnitude of amplitude stress, stress ratio, voids, fibre volume fraction etc.) that influence the fatigue life of a laminated composite. Several studies have been conducted to characterise UD laminates, see e.g. [33,34]. The characterisation related to fatigue studies includes determination of constitutive properties (e.g. $E_{11}, E_{22}, G_{12}$ and $\nu_{12}$), strength properties (e.g. tensile and compressive strength parallel and orthogonal to fibre direction as well as shear strength) and fatigue properties (e.g. S-N curves for different stress ratios). By characterising UD laminates it is possible to discard the influence of different layups. The derived properties can then be regarded as material properties for the basic building block of a MD laminate – the single UD ply. It is well established in the composite community that classical laminate theory (CLT) [35] provides accurate predictions of arbitrary layups based on information of UD constitutive properties. Several researchers have proposed fatigue models based on derived constitutive, strength and fatigue properties for UD plies as seen in e.g. the phenomenological models reviewed in [10] and in the more advanced progressive damage models [36–39]. A fundamental assumption in all of these models is that the fatigue properties derived for the UD laminate are representative for the case when the UD laminate is embedded in an MD laminate. The models then use stress based analysis from either CLT analysis or FE analysis to predict when plies fail. The influence of ply failure on overall performance of the laminate is then accounted for in the progressive damage models by empirical degradation rules involving several non-measurable empirical constants.

The fatigue damage evolution in MD laminates as reported in e.g. [15,18–20,40–42] is different from that of derived fatigue properties from UD laminates. An example of the damage mode observed in a UD laminate is shown in Figure 10(a). Unstable propagation of a single crack occurs in a laminate consisting entirely of UD plies, which is not accompanied by progressive stiffness degradation prior to final failure. When constraining plies are present, as is the case for UD plies embedded in MD laminates, initiation of several cracks and stable crack propagation (as shown in Figure 10(b)) are observed. These damage mechanisms lead to a progressive stiffness degradation of the laminate during the fatigue test. This contradicts the fundamental assumption used in the phenomenological models [10] and in the

progressive damage models [36–39], which may explain why the models in [10] were found to provide largely unsafe design guidelines and why progressive damage models [36–39] employ several empirical rules and require several non-measurable empirical constants. Furthermore, it is clear that fatigue tests on UD material cannot provide sufficient fatigue failure properties to model the progression of actual damage mechanisms in MD laminates as all damage modes are not activated.

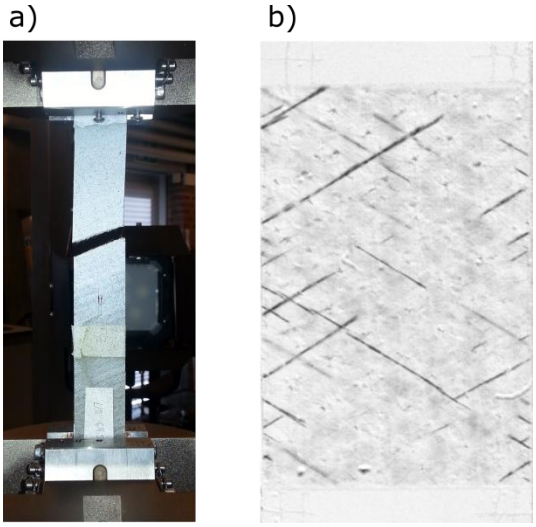


*Figure 10: Damage modes observed during fatigue test of laminated GFRP material for a) final failure of a UD laminate tested in an off-axis configuration and b) off-axis cracks in the 60° and -60° plies of a GFRP laminate with a layup given as [0/-60/0/60]s.*

Therefore, it was decided to quantify the fatigue damage evolution of the GFRP UD plies by embedding them in a laminate where they would be constrained by UD plies having another orientation. If the UD plies are oriented in an off-axis direction, it is possible to obtain multiaxial stress states and hence multiaxial fatigue test data from uni-axial testing due to the GFRP material anisotropy and the constraining effect of adjacent layers.

Experimental studies of fatigue damage in off-axis plies have been reported in several publications, see e.g. [15,18–20,40–42]. However, based on the literature review in (Paper #2) of these studies it was evident that there is a general agreement that the off-axis crack evolution can be described by initiation and the stable growth of cracks until a certain saturation point is reached. However, it was also clear that there is no general agreement on which fatigue properties should be derived or how they should be determined. Further on, all of these studies rely on manual and visual quantification of the off-axis crack evolution. Following the argumentation given in

Chapter 2, this way of obtaining data may be influenced by human error and thereby give biased results. Therefore, it was decided to use ACC for studying as well as quantifying the fatigue damage evolution of the GFRP material.

## 3.1. MATERIAL AND EXPERIMENT

The layup was chosen as $[0/-60/0/60]_s$ because this layup results in a multiaxial stress state in the off-axis plies. Further on, a similar layup had been tested on another material system and the results for those tests had been reported in [20]. These results could then serve as a qualitative benchmark of whether the same trends and mechanisms were observed. Twenty fatigue tests of this laminate were carried out, which included constant amplitude (CA) tension-tension (T-T) tests, variable amplitude (VA) block loading T-T tests and CA compression-tension (C-T) tests. Information about the tests is supplied in **Table 2**.

| Test Type | Maximum transverse normal stress in off-axis layer [MPa] | $F_{mean}$ [kN] | $F_{amp}$ [kN] | $R = \frac{F_{max}}{F_{min}}$ | Cycles | No. Tests |
|---|---|---|---|---|---|---|
| T-T CA | $\sigma_{22}^{max} = 69$ | 13.75 | 11.25 | 0.1 | $2 \cdot 10^4$ | 5 |
| T-T CA | $\sigma_{22}^{max} = 50$ | 10 | 8.2 | 0.1 | $1.1 \cdot 10^5$ | 5 |
| T-T CA | $\sigma_{22}^{max} = 39$ | 7.7 | 6.3 | 0.1 | $4.5 \cdot 10^5$ | 4 |
| T-T CA | $\sigma_{22}^{max} = 31$ | 6.2 | 5 | 0.1 | $1.6 \cdot 10^6$ | 2 |
| C-T CA | $\sigma_{22}^{max} = 37$ | 5.2 | 8.2 | -0.2 | $10^5$ | 2 |
| T-T VA | $\sigma_{22}^{max} = 39/50$ | 7.7 / 10 | 8.2 / 6.3 | 0.1 | $3.5 \cdot 10^5$ | 2 |

*Table 2: Definition of test series carried out for a [0/-60/0/60]s laminate.*

The tests were carried out in an Instron 8820 load frame with a 100 kN servo-hydraulic actuator operated in load control. The damage evolution was monitored using ACC, lock-in DIC [43] and extensometer. An image and a sketch of the experimental setup are provided in (Paper #2).

## 3.2. ANALYSIS OF CRACK DENSITY RESULTS

The results obtained from the fatigue test included the change in laminate stiffness obtained from lock-in DIC measurements and extensometer readings as well as the crack field for the images processed with ACC. First the obtained results for crack density evolution were studied. Secondly, ACC was extended with a data mining

approach such that initiation and stable crack growth of the developed off-axis cracks could be detected and quantified.

Crack density evolution curves were obtained for the front side -60° single plies and the double 60° plies, which are referred to as the *thin* and *thick layer* respectively. Results for the CA T-T tests are shown in Figure 11.

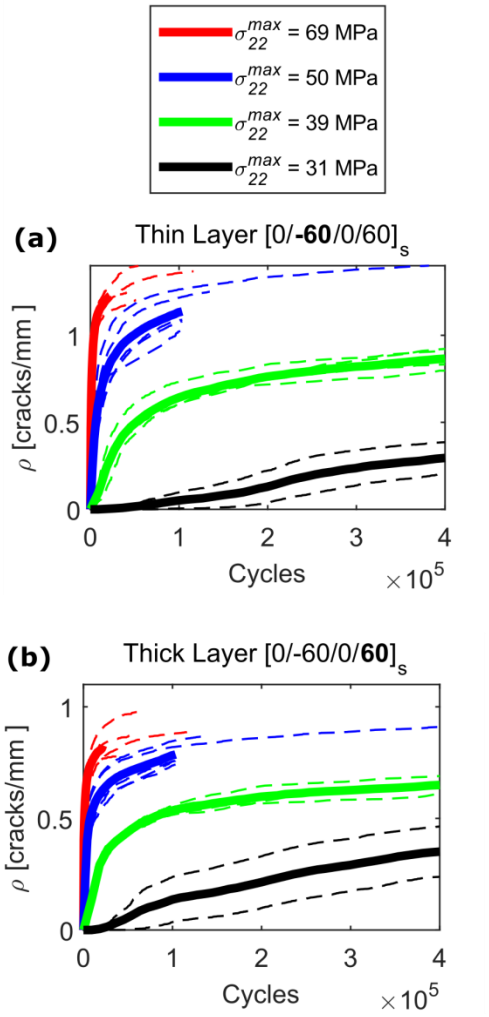


*Figure 11: Crack density measured using ACC during fatigue tests (T-T CA) for (a) the thin layer and (b) the thick layer. Dashed lines represent a single test and bold lines represent average crack density for each stress level (Paper #2).*

The results are consistent with the results reported in [20]. According to the idea of a Characteristic Damage State (CDS) [44], there can only be one saturation value for a particular layer. However, the slopes of the curves flatten, i.e. saturation, at a different stress levels, even though a clear asymptotic saturation is not achieved. Therefore a new terminology for this saturation value for each stress level was adopted by referring to it as the 'apparent saturation value'. The crack density observed for the *thick* layer is lower than the crack density observed for the *thin* layer. This occurs due to difference in the shielding effect as explained in (Paper #2).

The stiffness measured for the T-T CA tests is plotted in Figure 12.

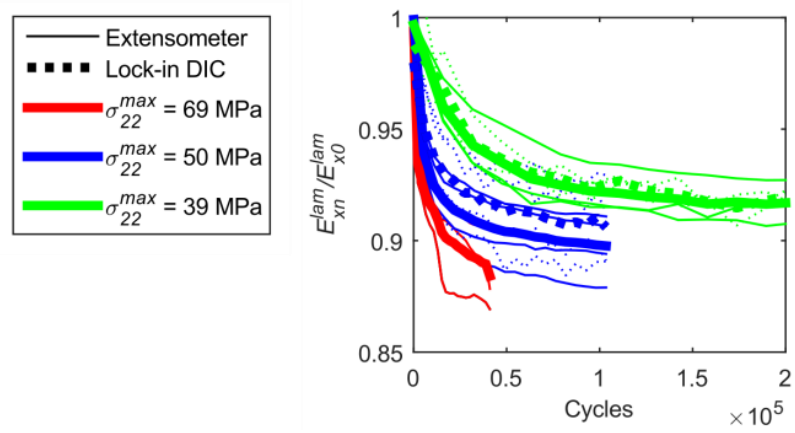


*Figure 12: Stiffness degradation during T-T CA tests monitored using lock-in DIC (dotted lines) and extensometer (full lines). Thin lines represent a single test and bold lines represent an average for all tests at a given load level (Paper #2).*

When the load is increased, the stiffness of the specimens decreases more rapidly and seems to saturate at different decreased levels. This agrees well with the crack density measurements in Figure 11 and is also supported by the results in [20]. As the material is loaded to a higher stress level, the crack density evolution rate increases along with the apparent saturation values.

It was decided to study how history dependent load effects influenced the crack density evolution in the laminate under VA T-T block loading to create benchmark results for the multiaxial fatigue model. Also, because it was not possible to find crack density evolution studies for VA T-T block loading in the open literature. Figure 13 shows the crack density measurements obtained from these VA T-T block loading tests.

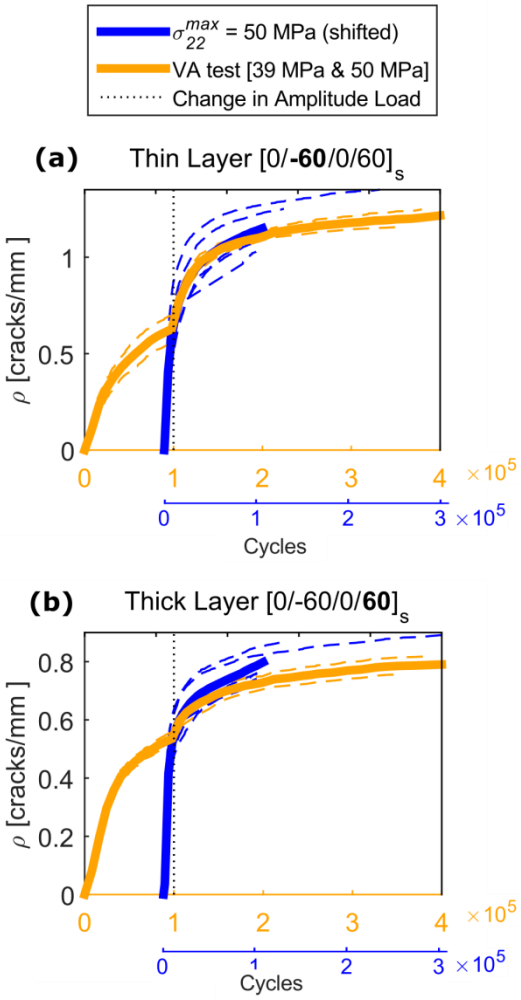


*Figure 13: Crack density measured during T-T VA fatigue tests compared to T-T CA fatigue tests at a stress level of 50MPa. The CA test results have been shifted such that the blue axis denotes the number of cycles. Dashed lines represent a single test and bold lines represent average crack density for each stress level (Paper #2).*

The crack density measurement from the 50 MPa CA T-T measurements is included for easy comparison. The results of the CA 50 MPa tests have been shifted $9 \times 10^4$ cycles so that the average crack densities of the VA and CA tests are the same at $10^5$ cycles, where the load in the VA test was increased from 39 MPa to 50 MPa. It was observed that the crack density evolution rate and apparent saturation level appeared to be identical for the two test series when the load was increased. This means that

crack density is a suitable damage measurement variable for defining load-history dependent effects, and the VA effect may simply scale linearly.

It was also decided to study the influence of C-T loading on crack density evolution as no results for the influence of C-T loading on crack density evolution in GFRP were available in the open literature in the beginning of this Ph.D project. A recent publication on the influence of C-T loading on the number of cycles to crack initiation and the crack growth rate can now be found in [45]. Crack density measurements from the C-T loading tests are given in Figure 14.

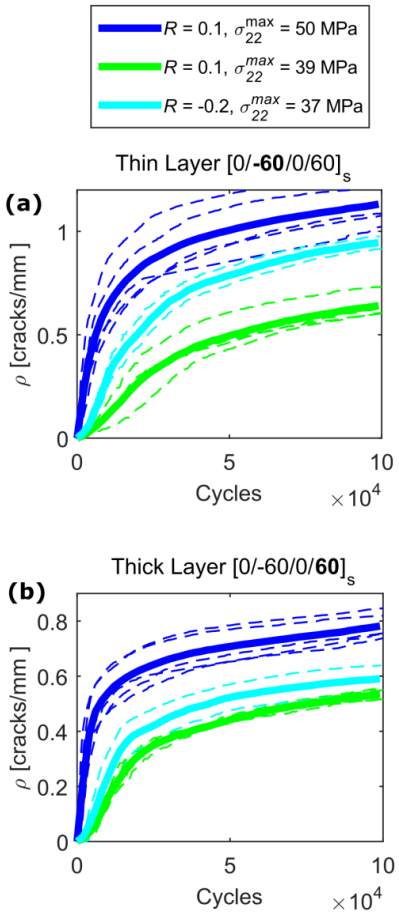


*Figure 14: Measured crack density for C-T CA fatigue tests compared to T-T CA fatigue tests. Dashed lines represent a single test and bold lines represent average crack density for each stress level (Paper #2).*

The 50 MPa CA T-T tests were subjected to the same load amplitude as the 37 MPa C-T tests. Based on the results it was observed that T-T loading results in a higher crack density evolution rate and apparent saturation value than C-T loading for the same load amplitude. This is in agreement with results reported in [45].

## 3.3. ANALYSIS OF CRACK INITIATION AND CRACK GROWTH

The off-axis crack density evolution consists of initiation and steady-state crack growth. ACC was extended to study these phenomena in more detail. The extension consisted of a computer code, which could data mine the crack field test information obtained from the ACC data acquisition method. The information extracted from the crack field data was chosen to be initiation and crack growth rates for isolated off-axis cracks. Isolated cracks refer to cracks, which have not felt the presence of other cracks until it initiates and while it grows. When the tests are carried out in load control, the stress at the location of the isolated cracks has not changed until the crack initiates. Therefore, fatigue material properties can be directly derived from data for initiation and crack growth of isolated cracks without imposing assumptions on damage accumulation for varying load histories.

To determine when off-axis cracks could be considered as isolated a unit-cell Finite Element (FE) model of the tested laminate was built. For a full description of the model see (Paper #2). Using the unit-cell model, it was found, that off-axis cracks could be considered isolated, as long as the location of crack initiation and the crack front was distanced four times the layer thickness away from other cracks. Cycles to initiation of isolated cracks for the different CA stress levels are shown in Figure 15.

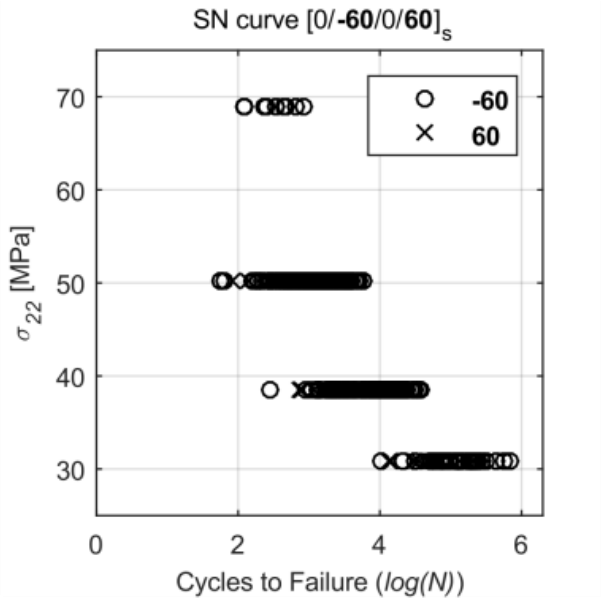


*Figure 15: S-N diagram for initiation of isolated off-axis cracks (Paper #2).*

The number of cycles to off-axis crack initiation varies over two decades and this highlights the large variability and thereby stochastic nature of the material tested. The fatigue off-axis crack initiation strength can therefore not be considered deterministic as e.g. the progressive damage evolution models ([36–39]) do. The stochastic nature of off-axis crack initiation should instead be modelled by a probability function.

The off-axis crack initiation data from Figure 15 were plotted in a normal and Weibull probability plots to identify, which probability function would model the stochastics of off-axis crack initiation satisfactorily. The obtained Weibull probability plots are shown in Figure 16.

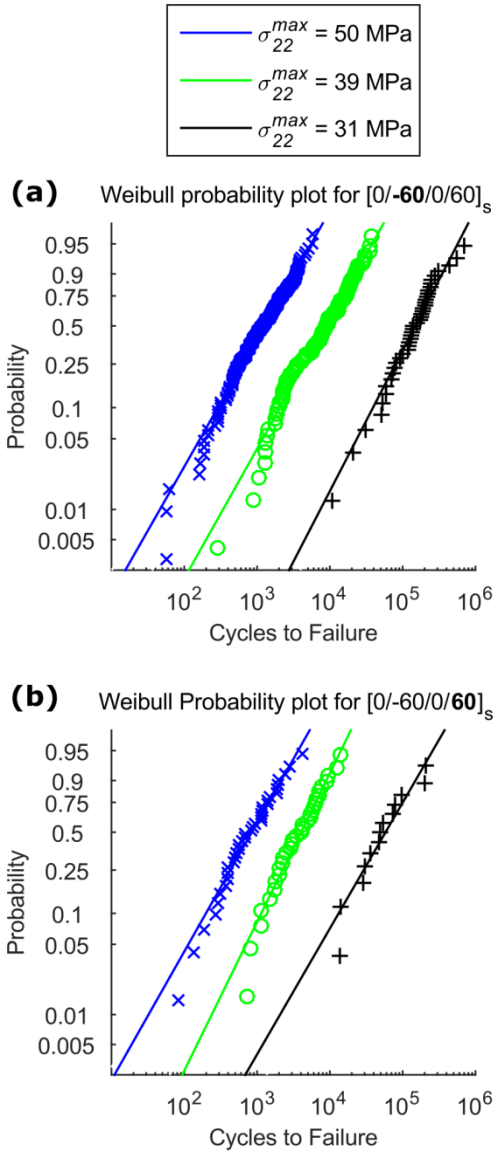


*Figure 16: Data for the initiation of isolated cracks from Figure 15 replotted in a Weibull probability plot (Paper #2).*

Linear trends in the dataset for both layers and all datasets are clearly observed and this was not the case when the data were analysed using the normal-probability plot. Therefore, it was concluded that the Weibull distribution describes the stochastic nature of the off-axis crack initiation well. Furthermore, statistical analysis as described in (Paper #2) showed, that the Weibull shape parameter was constant for

all tested stress levels and for both layers. The scale parameter was found to depend on the stress level, and this relation could be modelled by the classical S-N power law relationship given by:

$$S = S_0 N^k \quad \textbf{(1)}$$

where $S$ is the stress level (in this case chosen as $\sigma_{22}^{max}$), $N$ is the number of cycles to failure and $S_0$ and $k$ are empirical constants determined by fitting the S-N power law to experimental data. As described in (Paper #2), this means that it is possible to model the crack initiation process by a Weibull cumulative distribution function given as:

$$P_s(x,S) = 1 - \exp\left(-\left[\frac{x}{\left(\frac{S}{S_0}\right)^{1/k}}\right]^{\beta}\right) \quad (2)$$

where $\beta$ is the Weibull shape parameter and $x$ is a stochastic variable with the unit of number of cycles. The measured crack growth rates of isolated off-axis cracks obtained from the data mining are plotted in Figure 17 as function of the calculated Energy Release Rate (ERR).

Based on the results it is clear that the CGR increases with increasing ERR. This relationship is commonly referred to as the Paris' Law relationship and is given as

$$CGR = D \cdot {G_{tot}}^n \quad \textbf{(3)}$$

where $G_{tot}$ is the total ERR and $D$ and $n$ are empirical constants determined by fitting the Paris Law' to the experimental data. A large variance in the data is observed, and the magnitude of the variance is seen to be approximately the same as found in [46]. The observed variance indicates that a single Paris' Law relationship is not sufficient to describe the physics of crack propagation. Therefore, the measured Crack Growth Rates (CGR) were normalised using the fitted Paris Law and the normalised data was analysed using normal and Weibull probability plots. Based on this analysis it was found that the Weibull cumulative distribution function given by

$$P_c(CGR, G_{tot}) = 1 - \exp\left(-\left[\frac{CGR}{D \cdot {G_{tot}}^n}\right]^{\beta_c}\right) \quad (4)$$

where $\beta_c$ is the Weibull shape parameter, was suitable for modelling the stochastic nature of CGR. Furthermore, it was found that the Weibull shape parameter ($\beta_c$) was independent of the magnitude of the energy release rate.

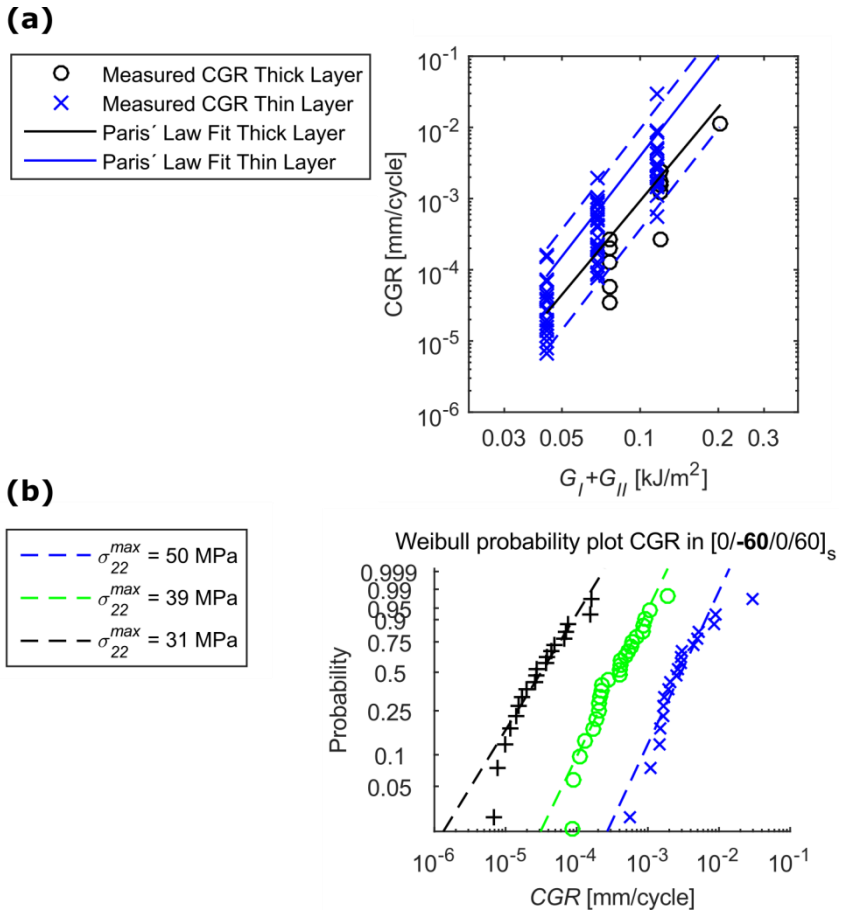


*Figure 17: a) crack growth rate as function of total ERR with Paris' Law relationship fitted to the data, where solid lines represent the fitted Paris Law and dashed lines represent the 95%-5% prediction interval. b) CGR data for the thin layer plotted in a Weibull probability plot where the dashed lines represent the fitted Weibull distribution for each stress level (Paper #2).*

## 3.4. CONCLUSIONS

The research conducted in connection with the quantification of the GFRP off-axis plies using ACC led to the following novel conclusions:

- Crack initiation and crack growth can be studied in greater detail than manual counting because the ACC approach for the first time makes it

feasible to detect and measure the crack evolution process throughout the entire fatigue test with sufficient temporal resolution (Paper #2).

- The crack density is a suitable damage measure for variable amplitude block loading, and T-T loading results in a higher crack density evolution rate and apparent saturation value than C-T loading for the same load amplitude (Paper #2).
- It is possible to efficiently derive the classical S-N relationship and Paris' Law like curves from the data obtained using the ACC approach and by fully accounting for crack interaction, so the nature and magnitude of the stress is established at every measurement and material point throughout the fatigue test providing an enhanced understanding of the causes of the damage progression (Paper #2).
- The Weibull distribution represents effectively the stochastic nature of isolated off-axis crack initiation and crack growth rate, and the Weibull parameters are derived directly, i.e. without resorting to inverse techniques, using ACC due to the data rich nature of the measurement method (Paper #2).
- The shape parameter of the Weibull distribution is independent of the applied stress and does not vary with ply thicknesses (Paper #2).

# CHAPTER 4. MICRO-MECHANICAL MODELS FOR PREDICTING STIFFNESS DEGRADATION

As shown in Chapter 3, the off-axis crack density evolution explains the stiffness degradation observed during the fatigue tests. The stiffness of the MD laminate decreases as the off-axis crack density increases. Furthermore, off-axis cracks result in stress redistribution in the damaged MD laminate, where stress in adjacent layers is increased and the stress in the damaged layer is decreased. The decrease of the stress in the damaged layers results in a shielding effect. The shielding effect impedes crack initiation and lowers the crack growth rate of propagating cracks. It is therefore important to both predict the stiffness degradation of the laminate as this can be used to assess if the overall structural requirements are met by the damaged laminate and to accurately predict the shielding effect as this is needed to describe the off-axis crack evolution process based on the derived fatigue evolution parameters.

Correlating the off-axis crack density with the stiffness degradation of an arbitrary MD laminate is essentially a 3D solid mechanics problem. In most cases, it is difficult or impossible to obtain an accurate analytical solution for this. The problem could be solved using FE based techniques but such an approach was disregarded as it is computationally heavy. Several analytical models for predicting the stiffness degradation based on the off-axis crack density have been proposed in the open literature e.g. [14,47–50]. The proposed models use simplifying assumptions to obtain predictions for the stiffness degradation of the laminate. Based on a literature review of available models it was decided to use the well-developed GLOB-LOC model [14,51–53]. The GLOB-LOC model was chosen because:

- Applies to arbitrary laminates
- Provide results for Crack Opening Displacement (COD) and Crack Sliding Displacement (CSD), which are used to compute the Mode I and Mode II ERRs according to the method described in [20]
- Accounting for crack interaction in terms of COD as presented in [52]
- Fast to compute
- Extendable framework as utilised in Paper #4, where the following tools have been developed and implemented in the model:
  - Accounting for crack interaction in terms of CSD
  - Recovery of the transverse normal stress and shear stress field between off-axis cracks

## 4.1. GLOB-LOC

The GLOB-LOC model belongs to the class of Crack Faces Displacement (CFD) models [48]. These types of models use the micro-mechanical theorem, which states that the volume average linear strains for a given layer are equal to the boundary-averaged linear strains:

$$E_{ij} = \frac{1}{V}\int_S \frac{1}{2}(u_i n_j + u_j n_i)dS \tag{5}$$

where $E_{ij}$ is the volume average strain tensor, $V$ is the volume, $S$ is the surface and $u_i$ is the displacement vector at the surface defined by the normal vector $n_j$. In the following a plane stress state will be assumed and the influence of out-of-plane transverse shear will be neglected. Therefore, only in plane strains are considered in relation to (5). The boundary-averaged in-plane strains include both the macroscopic laminate boundary surface and the internal off-axis crack surfaces. The boundary-averaged strains therefore consist of two parts and the equality from (5) for the k'th laminate layer can then be written as:

$$\begin{Bmatrix} \bar{\epsilon}_{11} \\ \bar{\epsilon}_{22} \\ \bar{\gamma}_{12} \end{Bmatrix}_k = \begin{Bmatrix} \epsilon_{11} \\ \epsilon_{22} \\ \gamma_{12} \end{Bmatrix}_{LAM} + \begin{Bmatrix} \beta_{11} \\ \beta_{22} \\ 2\beta_{12} \end{Bmatrix}_k \tag{6}$$

where $\bar{\epsilon}_{\alpha\beta}$ is the volume average strains, $\epsilon_{\alpha\beta}$ denotes the strains at the laminate boundary and $\beta_{\alpha\beta}$ denotes the Vakulenko-Kachanov tensor defined as:

$$\beta_{\alpha\beta} = \frac{1}{V}\int_{S_c} \frac{1}{2}(u_\alpha n_\beta + u_\beta n_\alpha)dS \tag{7}$$

where $s_c$ is the surface of internal crack faces. The volume average strains in (6) can then be determined using volume averaged equilibrium conditions and the constitutive relations for the material. The problem of determining the stiffness of the damaged laminate then becomes a problem of determining $\beta_{\alpha\beta}$ for each layer which is equivalent to determining the displacements of internal crack faces.

Figure 18 shows the geometry of a Representative Volume Element (RVE) with global coordinate system and the local material coordinate system for the cracked middle layer.

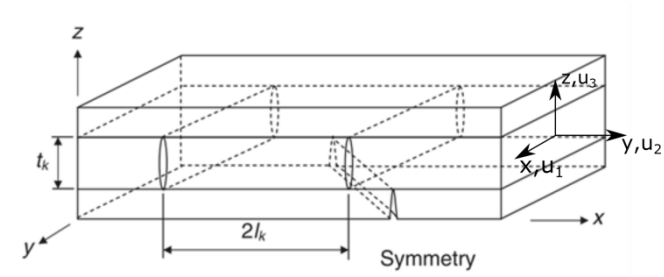


*Figure 18: Geometry of RVE used in derivation of the GLOB-LOC model* [52].

For in-plane loadings the displacements of crack faces in the middle layer consist of an opening displacement ($\Delta u_2$) perpendicular to the orientation of the fibres and a sliding displacement ($\Delta u_1$) parallel to the orientation of the fibres. It is generally a 3D problem to determine $\Delta u_1$ and $\Delta u_2$ since $\Delta u_1$ and $\Delta u_2$ are displacements in the xy-plane and are functions of the z-coordinate. However, since $\beta$ is a layer-surface-average it is only necessary to determine $\Delta u_1$ and $\Delta u_2$ averaged over the height of the cracked layer. The layer average displacements are defined as:

$$u_{1a}^k = \frac{1}{2t_k}\int_{-t_k/2}^{t_k/2} \Delta u_1(z)\, dz, \qquad u_{2a}^k = \frac{1}{2t_k}\int_{-t_k/2}^{t_k/2} \Delta u_2(z)\, dz \tag{8}$$

As described in [52], the layer average displacements are functions of the applied stress, the constitutive properties and the thickness of the damaged and the constraining layers. By using 3D finite element analysis, Lundmark and Varna [14,51–53] showed that the layer average crack face displacements for the case of non-interacting off-axis cracks could be described by master curves given as:

$$u_{1a}^k = \frac{u_{1an}^k t_k \sigma_{120}}{G_{12}}, \quad u_{2a}^k = \frac{u_{2an}^k t_k \sigma_{220}}{E_{22}} \tag{9}$$

where $\sigma_{120}$ and $\sigma_{220}$ are the in-plane shear and transverse normal stress in the k'th layer in the undamaged laminate, $G_{12}$ and $E_{22}$ are the shear and transverse Young's modulus of the k'th layer and $u_{1an}^k$ and $u_{2an}^k$ are given as:

$$u_{1an}^0 = A_1 + B_1\left(\frac{G_{12}}{G_{xy}^s}\right)^{n_1}, \quad u_{2an}^0 = A_2 + B_2\left(\frac{E_{22}}{E_{xx}^s}\right)^{n_2} \tag{10}$$

$G_{xy}^s$ and $E_{xx}^s$ are the shear modulus and the transverse Young's modulus of the constraining layers and $A_1$, $B_1$, $n_1$, $A_2$, $B_2$ and $n_2$ are empirical constants/functions of layer thickness derived from 3D FE analysis and are given in [53]. At high crack-densities the off-axis cracks become interacting and Lundmark & Varna [52,53]

proposed to use an interaction function to account for the interaction in the case of opening displacements:

$$u_{2an} = \lambda_k(\rho_k)u_{2an}^0 = tanh\left(\frac{0.84}{\rho_{kn}}\right)u_{2an}^0 \tag{11}$$

where $\rho_k$ denotes the crack density in the k'th layer and is defined as $\rho_k = \frac{\rho_{kn}}{t_k} = \frac{1}{2l_k sin(\theta_k)t_k}$ and $\rho_{kn}$ is called the normalised crack density. Lundmark & Varna [52,53] did not propose any method to account for the influence of off-axis crack interaction on the CSD. With $u_{1an}^0$ and $u_{2an}$ given by eqs. (10)-(11) the membrane stiffness of the damaged laminate is given by

$$[Q]^{LAM} = \left(I + \sum_{k=1}^{n} \frac{\rho_{kn}t_k}{h}[K(u_{1an}, u_{2an})]_k\,[S]_0^{LAM}\right)^{-1}[Q]_0^{LAM} \tag{12}$$

where $[S]_0^{LAM}$ and $[Q]_0^{LAM}$ are the compliance and stiffness matrices for the undamaged laminate, $h$ is the total laminate thickness and $[K(u_{1an}, u_{2an})]_k$ is a matrix function and is given in [53]. Eq. (12) represent the constitutive relation for a damaged laminate given by the GLOB-LOC model. It is important to note that it is a closed-form solution based on the empirical relations (9)-(11) for crack face displacements, hence fast to compute.

## 4.2. COMPARISON WITH STIFFNESS DEGRADATION MEASUREMENT

The GLOB-LOC model was implemented in a MATLAB laminate code to study the performance of the model and to use it for further development. It was chosen to benchmark the GLOB-LOC model against experimentally measured stiffness degradation obtained from the $[0/-60/0/60]_s$ laminate fatigue tests in (Paper #2). The only paper studying the GLOB-LOC models performance for fatigue damage was [27], who found that the GLOB-LOC model overestimates the stiffness of the damaged laminate. The crack density measurements obtained using ACC (Paper #1) were used as input to the GLOB-LOC model. The results from comparing the GLOB-LOC model with the experimentally measured stiffness are shown in Figure 19.

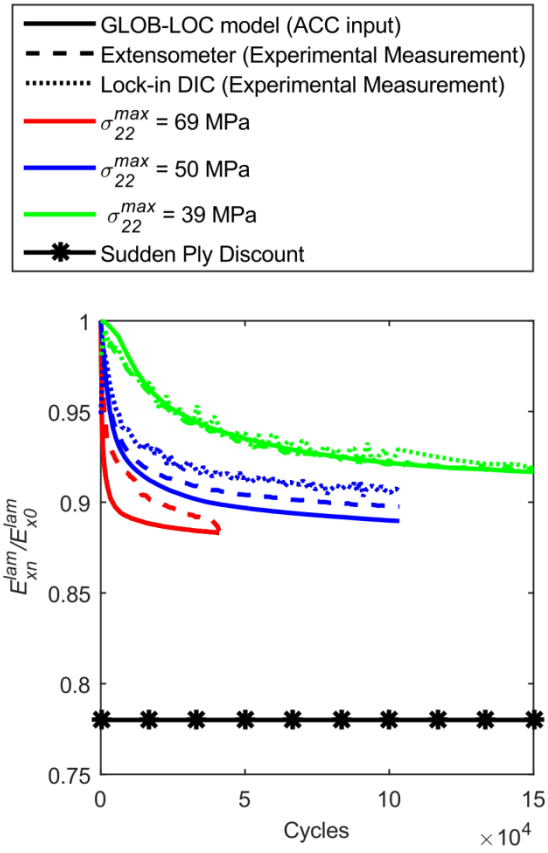


*Figure 19: Benchmark of stiffness degradation modelling using the GLOB-LOC model (based on ACC input) and the sudden ply discount degradation (Paper #2).*

As seen in Figure 19, the predictions of the GLOB-LOC and the measured stiffness agree well for fatigue induced off-axis cracks with a small underestimation of the laminate stiffness at high crack densities (red curve). The overestimation of laminate stiffness from [27] was not observed. Sisodia et. al [27] informed GLOB-LOC by crack densities measured by edge-examination, which may explain the overestimation if the edge crack density was not representative for the through width crack density. The sudden ply discount method from the progressive continuum damage model [36] was included in the benchmark as well, and it is seen that this degradation approach is overly conservative. The GLOB-LOC model therefore presents a much more accurate way of modelling fatigue damage than the sudden ply discount method. Since GLOB-LOC does not present means of describing the evolution of damage, it was decided for future research to extend the GLOB-LOC with the capabilities of modelling off-axis crack evolution under fatigue loading.

## 4.3. EXTENDING GLOB-LOC

Off-axis crack evolution in composite laminates is a multi-scale and hierarchical process, involving several length scales [54]. Off-axis crack initiation results from damage accumulation in the matrix material at the micro-scale, i.e. at the length scale of the inter-fibre spacing [54]. Off-axis crack propagation is controlled by micro-cracks in the matrix material ahead of the off-axis crack tip (Chapter 5 & Paper #3). The damage evolution rate for off-axis crack initiation and propagation is described by non-linear functions of the local stress state at the origin of damage (S-N and Paris' Law like relationships). In order to predict and model off-axis crack initiation and propagation it is therefore necessary to accurately compute the stress state at the location of the damage development.

GLOB-LOC in the form provided in [14,51–53] has some limitations, which make it difficult to use for describing off-axis crack evolution. As GLOB-LOC is based on volume and boundary averaging it is only possible to obtain stress/strain information averaged over the entire volume of each layer. The stress in a damaged layer varies between a stress free condition on the crack faces to a stress state equivalent to the one in the undamaged laminate, if the material point under consideration is distanced sufficiently far from off-axis cracks. Since the SN-relationship and the Paris' Law like relationship are non-linear it is not correct to use volume average stresses/strains. Further on, the GLOB-LOC model does not provide a way to account for CSD interaction at high intralaminar crack densities. CSD interaction is important to take into consideration when accurately determining the local multiaxial stress state and the local mixed-mode loading condition ([54], Paper #3). It was therefore decided to extend GLOB-LOC in the present project with a way to model CSD interaction and to obtain the variations in the stress field within a damaged layer.

Parametric 3D FE analysis of a cross-ply laminate was carried out for the CSD interaction. The COD and the CSD as function of the crack density were derived from the model for different constraining layer thicknesses. The FE model used to study the COD interaction was similar to the model given in [52] and the derived results are given in Figure 20(a). The results from Figure 20(a) agree with the results from [52], which thereby validate the FE-model developed in the current project. The same model, but with CSD boundary Conditions as described in (Paper #4) was then used to determine the CSD interaction function. The derived CSD as function of crack density for different constraining layer thicknesses are shown in Figure 20(b). Based on these results it was found that the CSD when crack interaction was presented can be modelled by:

$$u_{1an} = \lambda_k(\rho_k) u_{1an}^0 = tanh\left(\frac{1.3}{\rho_{kn}}\right) u_{1an}^0 \; for \; \sigma_{22} > 0 \qquad (13)$$

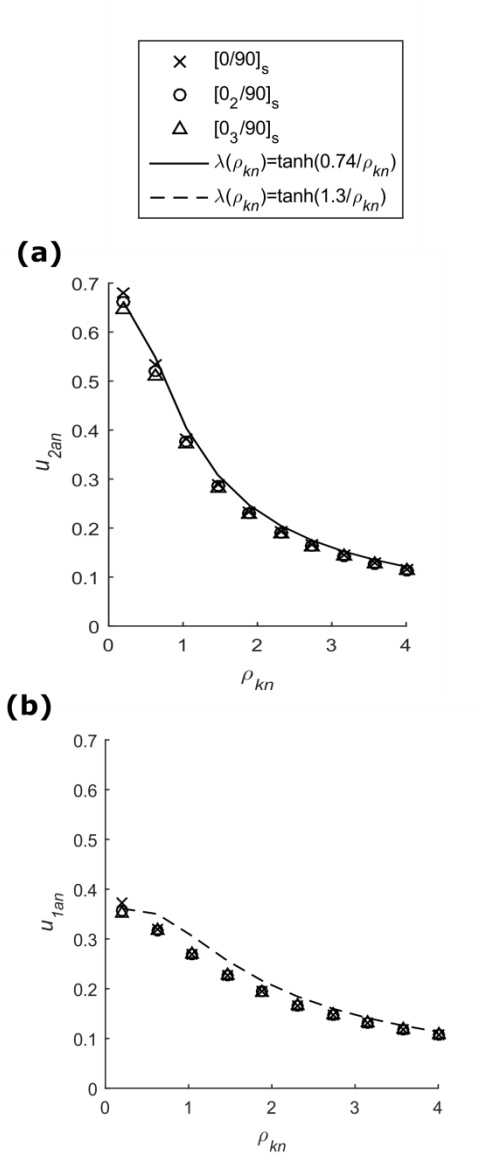


*Figure 20: (a) Normalised COD and (b) normalised CSD for different constraining effect as function of normalised crack density (Paper #4).*

It is also important to be able to compute the stress between off-axis cracks because the local stress state defines how damage progresses. The average stress in a cracked layer depends on the COD and CSD in the cracked layer. The average transverse

normal stress ($\sigma_{22}$) in the cracked layer can be obtained as described in [55] and can be computed as:

$$\sigma_{22,avg}^{k} = k_{\sigma 2}\sigma_{220}^{k} = \left(1 - 2u_{2an}(\rho_{kn})\rho_{kn}\frac{t_k t_s E_T^S}{E_{T0}^{LAM}\left(\frac{t_k}{2} + t_s\right)}\right)\sigma_{220}^{k} \qquad (14)$$

where $E_{T0}^{LAM}$ is the initial 'average' modulus of the whole laminate (CLT) in the undamaged condition, $t_s$ is the average thickness of the sub-laminates and $E_T^S$ is the average Young's modulus of the top and bottom sub-laminate perpendicular to the off-axis crack as defined in [53].

In (Paper #4) the average shear stress ($\tau_{22}$) as function of the CSD is derived by considering cracked layers separately and assuming the laminate configuration to be symmetric and balanced. Using force equilibrium conditions and macroscopic strain compatibility of the laminate layers it turns out that the average shear stress is given by:

$$\tau_{12,avg}^{k} = k_{\sigma 1}\tau_{120}^{k} = \left(1 - 2u_{1an}(\rho_{kn})\rho_{kn}\frac{t_k t_s G_T^S}{G_{T0}^{LAM}\left(\frac{t_k}{2} + t_s\right)}\right)\tau_{120}^{k} \qquad (15)$$

where $G_T^S$ is the average shear-modulus of the top and bottom sublaminate, $G_{T0}^{LAM}$ is the initial shear modulus of the whole laminate (CLT) in the undamaged condition and $t_s$ is the thickness of the sublaminate on either side of the cracked layer.

As described in [56] the stress averaged through the thickness of the cracked layer can be described using a shear lag solution which for the $\tau_{12}^{k}$ will be given by as:

$$\tau_{12}^{k}(\xi) = \tau_{120}^{k}\left(1 - \frac{cosh(\Phi_1 \xi)}{cosh\left(\frac{\Phi_1}{2\rho_{kn}}\right)}\right) \qquad (16)$$

where $\tau_{120}^{k}$ is the stress in the undamaged laminate, ξ is non-dimensional coordinate and Φ is an unknown constant dependent on the material properties and laminate configuration. Setting eq. (15) equal to the volume average of the shear lag solution as:

$$\tau_{12,avg}^{k} = k_{\sigma 1}\tau_{120}^{k} = \frac{\tau_{120}^{k}}{\rho}\int_{-\frac{1}{2\rho t_k}}^{\frac{1}{2\rho t_k}}\left(1 - \frac{\cosh(\Phi_1 \xi)}{\cosh\left(\Phi_1 \frac{1}{2\rho_{kn}}\right)}\right)d\,\xi \qquad (17)$$

then $\Phi_1$ is the only unknown parameter and can hence be determined. To validate this approach the stresses were computed using the now modified GLOB-LOC model and derived using the 3D FE unit-cell model as described in (Paper #4). The results obtained from both models are shown in Figure 21.

It is clearly seen that the stress field is accurately recovered, which is needed to compute the local damage evolution rate at different locations within the laminate where off-axis cracks might initiate and propagate. Furthermore, it should be noted that the results presented in this section also serve as a validation of the implementation of the modified GLOB-LOC model.

## 4.4. CONCLUSIONS

The research conducted in connection with modelling the stiffness degradation using the GLOB-LOC model led to the following conclusions:

- The GLOB-LOC model slightly under predicts the stiffness of the degraded laminate whereas the sudden ply discount policy under-predicts the stiffness by a large margin indicating that the sudden ply discount approach is not suitable for modelling fatigue damage (Paper #2).
- The effect of crack interaction on the CSD at high intralaminar crack densities can be accounted for by the interaction function in eq. (13) for GFRP laminates with different constraining effects when no compressive stresses are acting on the crack faces.
- The GLOB-LOC model has been extended such that the varying stress field within the damaged layer can be recovered from the volume average properties obtained from the original GLOB-LOC model.

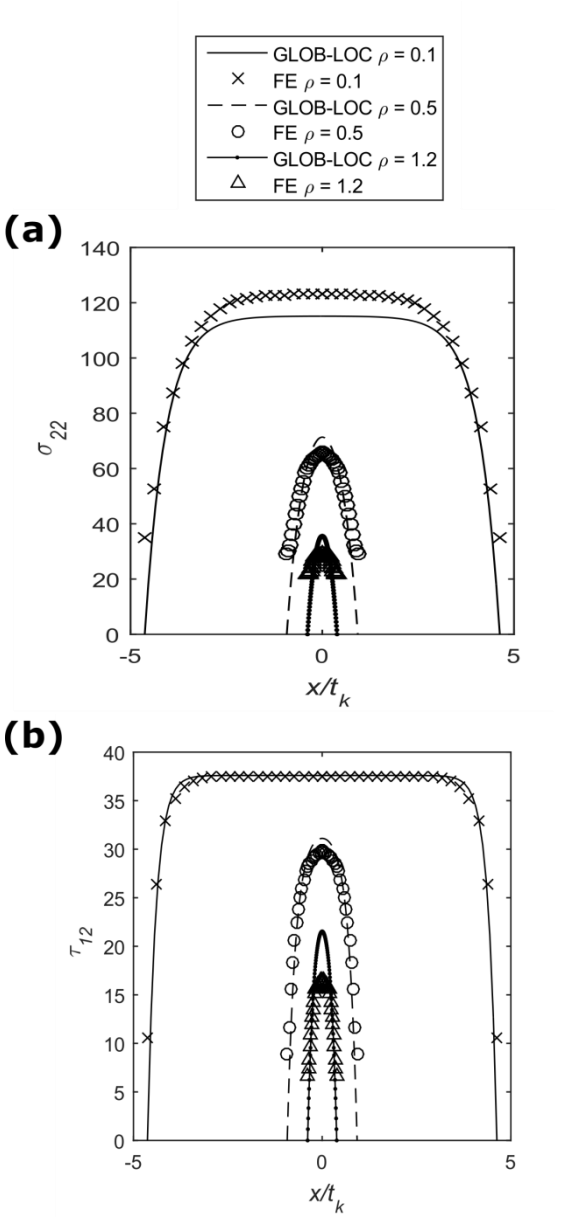


*Figure 21: a) transverse normal stress field and b) shear stress field between off-axis cracks for different crack densities for a [0/90]s layup and 1% strain applied (Paper #4).*

# CHAPTER 5. A MIXED-MODE PROPAGATION MODEL FOR OFF-AXIS CRACKS (PAPER #3)

Based on the successful validation and extension of GLOB-LOC, it was decided to develop an off-axis crack damage evolution model using only the information provided by the GLOB-LOC model. Recently, Carraro and Quaresimin [57] developed a physically based multiaxial evolution model for off-axis crack initiation based on damage modes observed on the micro-scale. Two different damage modes were observed at the micro-scale, where one damage mode was a micro crack parallel to the fibres and close to the interface and the other damage mode was a shear cusp crack. Carraro and Quaresimin [57] proposed that the Local Hydrostatic Stress (LHS) is responsible for the micro cracks parallel to the fibres, and the Local Maximum Principal Stress (LMPS) is responsible for the shear cusp cracks. The damage evolution rate as function of the stress level is based on an SN relationship for each damage mode. This means that in order to use the model, the composite material has to be fatigue tested in two different multiaxial stress conditions where each damage mode is activated. Hence, the model requires a very limited experimental campaign to characterise the material and it is physically based such that it is generally applicable to different multiaxial stress states. It was decided to use the model from [57] to predict and model the initiation of off-axis cracks, since the model can be evaluated using information obtained from the GLOB-LOC model.

For the propagation part of the evolution process, the open literature was searched for physically based models capable of predicting the CGR. The CGR depends on the magnitude of the applied load, the geometry of the crack and the mode-mixity [58]. The literature survey is given in (Paper #3), and from this survey it is clear that no physical based models suitable for describing off-axis crack propagation under mixed-mode loading conditions were available in the open literature. Prof. Marino Quaresimin and his research group at the University of Padova were also searching for a similar model for their research activities and therefore it was decided to develop a model as a joint effort. The requirements for the model were defined to be:

- Physically based such that it describes the actual damage modes observed in experiments.
- Computationally efficient, meaning that it should be possible to evaluate the model using only information provided by micro-mechanical models (as e.g. the GLOB-LOC model).

- The required experimental campaign to determine evolution parameters should be less or equivalent to the campaign required to calibrate the off-axis crack initiation model [57].

The model was mainly developed during the external research stay at the University of Padova and is briefly described in the following.

## 5.1. MODEL

As described in Chapter 3, the CGR can be modelled by a Paris' Law like relationship. However, the CGR also depends on the local mode-mixity [58] and the CGR decreases for constant total ERR when the local mode-mixity increase. The local mode-mixity is defined as: $MM = \frac{G_{II}}{G_I+G_{II}}$. This increased resistance to crack growth can be explained by different underlying damage mechanisms responsible for crack propagation. From a literature survey of damage modes observed during crack propagation or post mortem fracture surface analysis in thermoset polymer matrix materials, it was found that in general several different fracture features have been reported [59–63]. These different features are scarps, ribbons, tilted layered cracks and cusps. The features are present due to a series of events in the process zone ahead of the off-axis crack. Micro-voids form in the process zone in front of the off-axis crack tip due to the high local stress resulting from the presence of the off-axis crack tip. The micro-voids eventually coalesce and form scarps, ribbons, tilted layered cracks or shear cusps. When the scarps, ribbons, tilted layered cracks and shear cusps are sufficiently developed, they coalesce with the off-axis crack and this coalescence leads to crack propagation. This sequence is sketched in Figure 22.

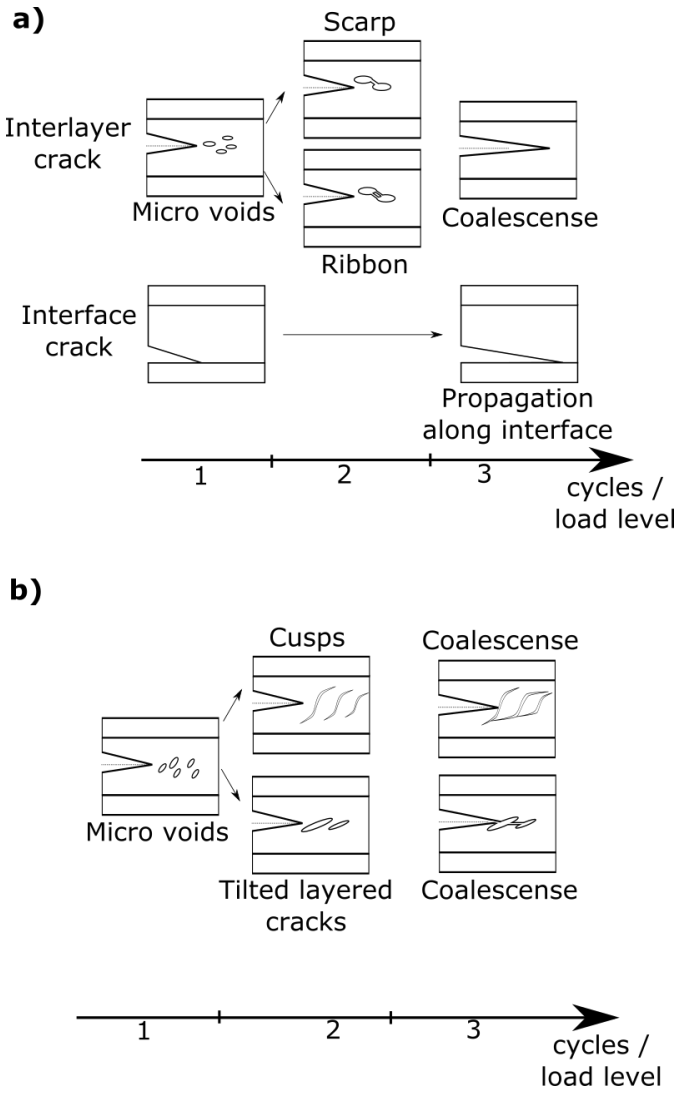


*Figure 22: Reported damage sequence for a) Mode I dominated loading and b) Mode II dominated loading.*

Scarps and ribbons are usually observed when the local mode-mixity is close to pure Mode I and tilted layered cracks are observed when a significant amount of Mode II loading is present as well [54,59–61]. An important part of the crack propagation process is the series of initiation events ahead of the crack tip in the failure process zone. As scarp, ribbons, tilted layered cracks and shear cusps represent similar

features as observed for off-axis crack initiation [57] and their occurrence is a result of the local stress state in front of the crack, it was decided to use the magnitude of the LHS and LMPS in the matrix in front of the off-axis as measures for describing the off-axis CGR.

However, to compute the LHS and LMPS in the process zone represent a 3D multi-scale problem, since the LHS and LMPS depends on the crack geometry, the constraining effect of adjacent layers, the local mode-mixity and the micro-scale geometry. Therefore, a part of (Paper #3) represents a multi-scale approach to obtain the LHS and LMPS in the process zone based on information obtained from micro-mechanical models. It is not known at which distance the off-axis cracks initiates, and therefore the magnitude of LHS and LMPS controlling crack propagation are formulated in terms of equivalent ERRs derived from the stress intensity factors (SIFs) for the off-axis crack (Paper #3). The proposed equivalent ERRs are:

$$G_{eq}^{LHS} = G_I = MM \cdot G_{tot} \tag{18}$$

$$\begin{aligned} G_{eq}^{LMPS} &= \left(\sqrt{MM} + \sqrt{1 - MM}\right)^2 \cdot (G_I + G_{II}) \\ &= \left(\sqrt{MM} + \sqrt{1 - MM}\right)^2 \cdot (G_{tot}) \end{aligned} \tag{19}$$

where $G_{tot}$ and $MM$ can be directly obtained from the GLOB-LOC model. The equivalent ERRs from Eqs. (18) and (19) are used to derive two Paris' Law relationships for the tested material. The Paris' Law relationships are used to predict the CGRs for any local mode-mixity and failure mode. The Paris' Law predicting the highest CGR is used to predict the crack density. The transition between the derived Paris' Laws has been found to be in good agreement with the transition of the observed damage modes on the microscopic scale (Paper #3), indicating that the model is in agreement with the physical damage evolution. Further on, it should be noted that the model does not require extensive testing to derive evolution parameters, since the two required Paris' Law curves can be derived from the same tests used to derive the SN-curves required for the initiation model from [57].

## 5.2. RESULTS

To illustrate the general applicability of the physically based model several data sets from the literature were analysed using Eqs. (18) and (19). (Paper #3) presents the results from using the model on off-axis crack propagation data from [58] and data for delamination in 0°/0° layer interfaces from [64,65]. The results from using the model on off-axis crack propagation data from [58] are also shown in Figure 23, where the crack propagation data is plotted in terms of $G_{tot}$, $G_{eq}^{LHS}$ and $G_{eq}^{LMPS}$ and Paris' Law like relationships have been fitted to the data for Mode I ($MM = [0; 0.26]$) and Mode II ($MM = ]0.26; 1]$) dominated propagation.

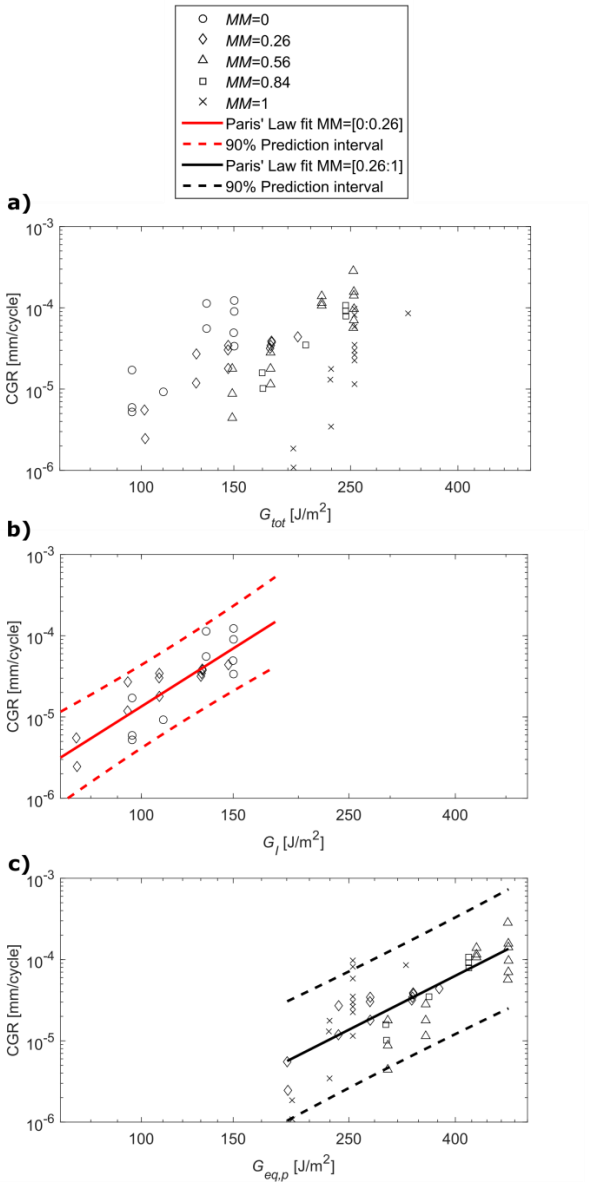


*Figure 23: CGR data for off-axis cracks in glass-epoxy tubes* [58]. *a) CGR data plotted as function of* $G_{tot}$. *b) CGR data plotted as function of* $G_I = G_{eq}^{LHS}$ *with a Paris' Law like relationship fitted to data for MM=[0:0.26] (red). c) CGR data plotted as function of* $G_{eq,p} = G_{eq}^{LMPS}$ *with a Paris' Law like relationship fitted to data for MM=]0.26:1] (black) (Paper #3).*

When the Paris' Law like relationships are fitted to the data plotted in terms of $G_{eq}^{LHS}$ for $MM = [0; 0.26]$) and $G_{eq}^{LMPS}$ for $MM = ]0.26; 1]$, the obtained 90% prediction interval is close to the inherent material scatter and this is not the case when Paris' Law like relationships are fitted to the CGR data in terms of $G_{tot}$. This shows that the model accurately accounts for the influence of local mode-mixity on the CGR for the entire range of local mode-mixities. The same performance of the model was found for the delamination data in [64,65] as reported in (Paper #3) but also in the case of bonded joints with data taken from [59,66], where data from [66] is reanalysed in Figure 24.

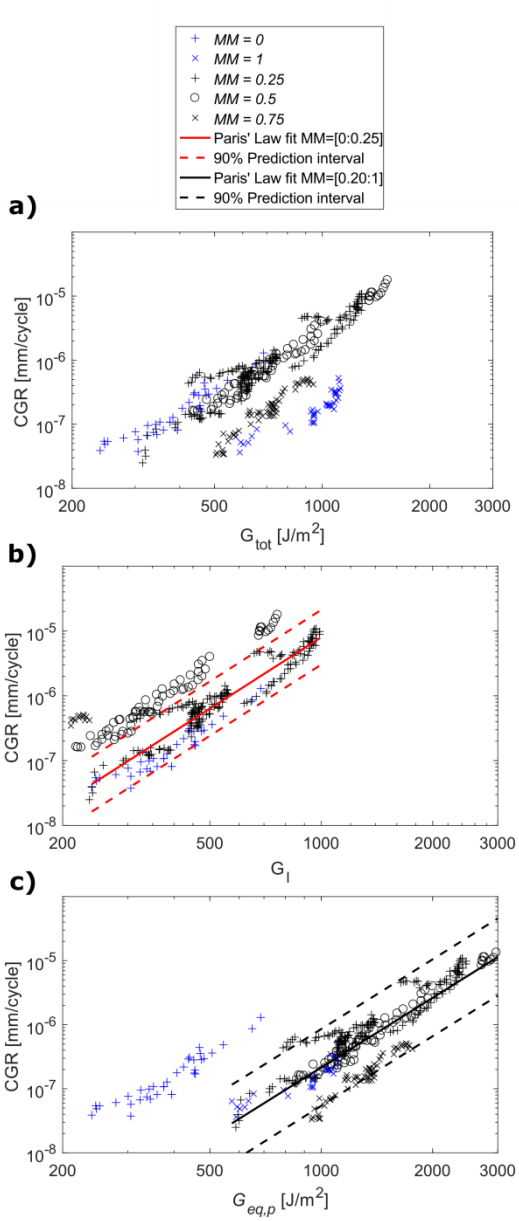


*Figure 24: CGR data for off-axis cracks in adhesive joints* [66]. *a) CGR data plotted as function of* $G_{tot}$. *b) CGR data plotted as function of* $G_I = G_{eq}^{LHS}$ *with a Paris' Law like relationship fitted to data for MM=[0:0.25] (red). c) CGR data plotted as function of* $G_{eq,p} = G_{eq}^{LMPS}$ *with a Paris' Law like relationship fitted to data for MM=]0.25:1] (black).*

## 5.3. ACCOUNTING FOR THE STRESS RATIO INFLUENCE

Since crack propagation is a series of damage modes resembling those of initiation, it is expected that changing the stress ratio will have the same influence on CGR as shown for initiation. To model the influence of load ratio on the number of cycles to off-axis crack initiation [67] proposed an empirical normalisation principle:

$$\psi = \frac{\sigma_a}{\sigma_s - \sigma_m} = \frac{\frac{1-R}{2}\sigma_{max}}{\sigma_s - \frac{1+R}{2}\sigma_{max}} = \frac{(1-R)\sigma_{max}}{2\sigma_s - (1+R)\sigma_{max}} \quad \textbf{(20)}$$

where $\sigma_a, \sigma_m, \sigma_{max}$ and $\sigma_s$ are the stress amplitude, the mean stress, the max stress and the ultimate tensile strength, respectively, and the stress ratio is given by $R = \frac{\sigma_{min}}{\sigma_{max}}$. In [68] it was demonstrated that if the stress measures used in Eq. (20) were LHS and LMPS, it would collapse off-axis crack initiation for glass-epoxy tubes from [45] into two master curves.

Assuming that a change in load ratio does not change the type of damage mechanisms in the process zone of the off-axis crack, then Eq. (20) can be rewritten in terms of $K_h$ and $K_p$ (as defined in Paper #3). The modification of Eq. (20) is then given as:

$$\varphi = \frac{K_f^a \frac{1}{\sqrt{2\pi r}}}{K_f^S \frac{1}{\sqrt{2\pi r}} - K_f^m \frac{1}{\sqrt{2\pi r}}} = \frac{\left(1 - R_f\right) K_f^{Max}}{2K_f^S - (1+R_f)K_f^{Max}} \quad (21)$$

where subscript $f = h$ or $p$, $K_f^S$ is the equivalent SIF resulting in quasi static failure and hence unstable crack growth and $R_f = \frac{K_{min}}{K_{max}}$. Expressing Eq. (21) in terms of the equivalent ERRs given in Eqs. (18)-(19) give:

$$\varphi^{\mathrm{d}} = \frac{(1 - R_c^d)\sqrt{G_{max}^d}}{2\sqrt{G_q^d} - (1 + R_c^d)\sqrt{G_{max}^d}} \quad \textbf{(22)}$$

where $d$=LHS or LMPS and $G_{max}^d$ is the maximum equivalent ERR for the active damage mode that controls the crack propagation. The reference stress ratio $R_c^d = \frac{\sqrt{G_{min}^d}}{\sqrt{G_{max}^d}}$ for each unique damage mode $d$ and $G_q^d$ is equivalent to the ERR

required for unstable crack propagation for each damage mode. Relating $G_q^d$ directly with the measured quasi-static ply strength is virtually impossible, since it would require a precise knowledge about the initial conditions of the defect that initiates the off-axis crack. Instead $G_q^d$ can be experimentally derived by defining the load at which an off-axis crack with a length that gives a steady-state ERR starts to propagate in an unstable manner. Data for e.g. $G_q^{LMPS}$ is not available in [68], but the static initiation strength of the material $\sigma_s^{LMPS}$ is provided. Assuming that increasing the load in an undamaged laminate to $\sigma_s^{LMPS}$ leads to unstable crack propagation for a crack length longer than the one required to reach the steady-state ERR, then

$$G_{CGR,Max}^{LMPS} < G_q^{LMPS} \leq G_{S,Max}^{LMPS} \quad \textbf{(23)}$$

where $G_{CGR,Max}^{LMPS}$ is the maximum equivalent ERR where stable crack propagation is observed and $G_{S,Max}^{LMPS}$ is the maximum equivalent ERR at quasi-static crack initiation.

From the static strength reported in [68] $G_{S,Max}^{LMPS}$ can be derived to $G_{S,Max}^{LMPS} = 1.37\ kJ/m^2$. The highest value of $G_{CGR,Max}^{LMPS}$ for the same material is found in tests of the flat $[0/50_2/0/\text{-}50_2]_s$ laminate in [20] and from these data can be computed to $G_{CGR,Max}^{LMPS} = 0.98\ kJ/m^2$.

In [45] the same material as tested in [68] and [20] has been tested at different stress ratios. The CGR data obtained from [45] for two different stress ratios is plotted in Figure 25(a). The same data is plotted in Figure 25(b) and Figure 25(c) in terms of $\varphi^{LMPS}$ according to Eq. (22) using the assumption that $G_q^{LMPS} = G_{S,Max}^{LMPS}$ in Figure 25(b) and the assumption that $G_q^{LMPS} = G_{CGR,Max}^{LMPS}$ in Figure 25(c). The data points in Figure 25(b) and Figure 25(c) are fitted with a Paris' Law given by $CGR = \varphi_0^{LMPS} \cdot (\varphi^{\mathrm{LMPS}})^{n^{LMPS}}$. As previously, the range of the prediction interval when $G_q^{LMPS} = G_{S,Max}^{LMPS}$ is similar to the scatter in the material data. This is not the case when $G_q^{LMPS} = G_{CGR,Max}^{LMPS}$ as seen in Figure 25(c), since the range of the prediction interval is considerably wider than the scatter in the material data.

Therefore, it can be concluded that the empirical normalisation principle from [67] in the modified version given in Eq. (22) can be used to model the influence of varying stress ratio on the CGR of off-axis cracks if $G_q^{LMPS} = G_{S,Max}^{LMPS}$ for the material tested, but importantly as $G_q^{LMPS}$ was not determined with high accuracy it also indicates that further investigations (and more tests) are needed to determine the value of $G_q^{LMPS}$ more accurately in order to generally validate the approach.

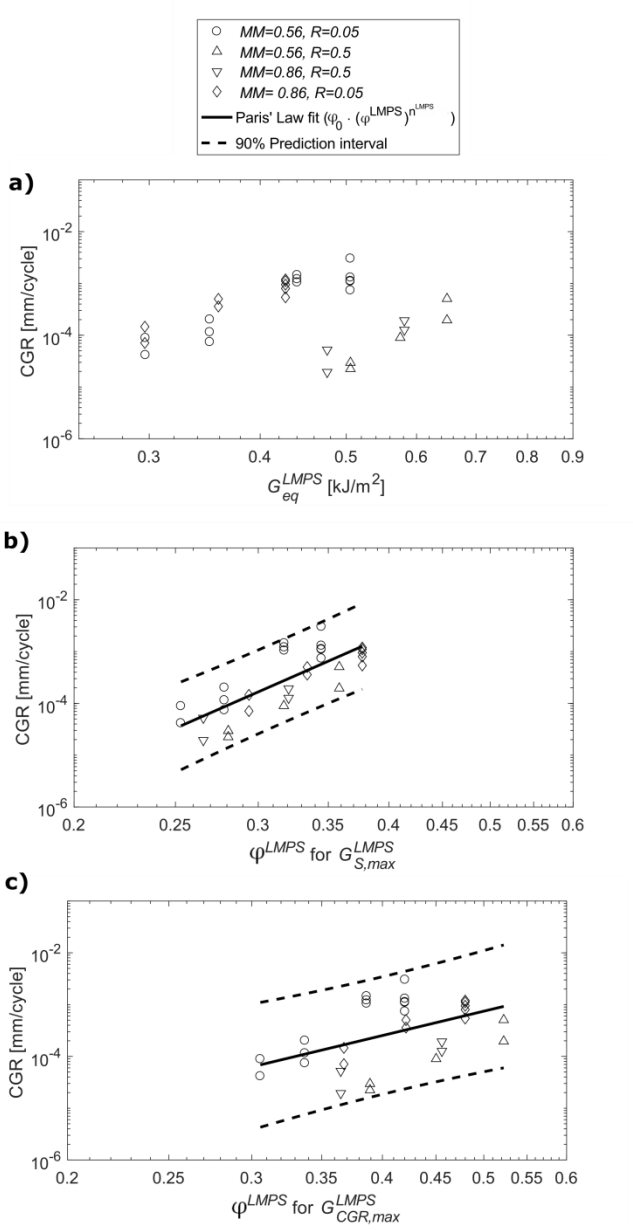


*Figure 25: CGR data for off-axis cracks in glass-epoxy tubes for varying stress ratio and mode-mixity obtained from* [45]. *a) CGR data plotted as function of $G_{eq}^{LMPS}$. b) CGR data plotted as function of $\varphi^{LMPS}$ using $G_{S,Max}^{LMPS}$ for normalisation and c) CGR data plotted as function of $\varphi^{LMPS}$ using $G_{CGR,Max}^{LMPS}$ for normalization.*

## 5.4. CONCLUSIONS

The research conducted in connection with modelling the mixed-mode crack propagation under fatigue led to the following novel conclusions:

- A novel physically based model for mixed-mode crack propagation in composite materials has been established.
- The local stress state in the failure process zone defines the type of damage modes responsible for crack propagation.
- The model is multi-scale and computationally efficient as it can be evaluated using only the information available in micro-mechanical models.
- The derivation of evolution parameters requires the same test campaign as used in the initiation model from [57], which means that only few tests are needed to obtain evolution parameters describing the off-axis crack evolution process.

# CHAPTER 6. A MULTIAXIAL FATIGUE MODEL FOR OFF-AXIS CRACK EVOLUTION (PAPER #4)

In line with the overarching aim of the Ph.D. project, the last part of the project was to develop a physically based multiaxial fatigue model for off-axis crack evolution. At this instant in the project, an efficient material characterisation method had been developed, the implementation of GLOB-LOC in an in-house code had been validated, GLOB-LOC had been extended to provide necessary information about the damaged laminate and lastly a physically based mixed-mode propagation model had been proposed. All the constituents deemed necessary to propose a physically based model of the off-axis crack evolution process were thereby in place.

Four models to predict off-axis crack evolution in composite laminates subjected to fatigue loading have been identified in the open literature [68–71]. The models proposed in [69–71] all describe off-axis crack evolution solely based on initiation strength. Therefore, none of the models account for the influence of multiaxial loads and the crack propagation aspect of the evolution process. Carraro [68] proposed an off-axis evolution model considering both the initiation and propagation of off-axis cracks. The model showed good agreement between the predicted and experimentally measured crack density evolution. However, the model is computationally expensive in terms of both memory and CPU-time as it is based on a full Monte-Carlo simulation of the evolution process. Further on, some of the parameters used in the model had to be determined from inverse modelling of the crack density evolution curves, which questions whether the determined parameters are material properties or ‘fitting’ parameters.

Therefore, it was decided to develop a new mechanistic model with the following requirements guiding the development:

- Use only physically based models for initiation, crack propagation and damage description.
- Capability of predicting crack density evolution in composite laminates subjected to multiaxial loads at different load ratios.
- Computationally efficient by adopting simplifying description of the crack field.

## 6.1. MODEL

As described in (Paper #2) the off-axis crack evolution process shows a deterministic dependence on influencing factors such as stress level and constraining effect, but the process is also stochastic. The deterministic influence of stress level and stress ratio on initiation of off-axis cracks for each damage mode can be described by a normalised SN-curve [57,68] given as

$$\psi^d = \psi_0^d \cdot \left(N_{fat}\right)^{m^d} \quad \text{for d} = \text{LHS, LMPS}$$
$$\text{with } \psi^d = \frac{(1-R_s^d)\sigma_{max}^d}{2\sigma_q^d-(1+R_s^d)\sigma_{max}^d} \quad \text{valid for } R_s^d > 0 \tag{24}$$

where $\sigma_q^d$ is the static strengths, $N_{fat}$ is the number of cycles to failure, $R_s^d = \frac{\sigma_{min}^d}{\sigma_{max}^d}$ and $\psi_0^d$ and $m^d$ are fitting parameters for the normalised SN Power law relationships. The deterministic influence of stress level, stress ratio and constraining effect on CGR for each propagation damage mode can be described by a Paris like law (Paper #3) as:

$$CGR^d = \varphi_0^d \cdot (\varphi^d)^{n^d} \quad \text{for d = LHS, LMPS}$$
$$\text{with } \varphi^d = \frac{(1-R_c^d)\sqrt{G_{max}^d}}{2\sqrt{G_q^d}-(1+R_c^d)\sqrt{G_{max}^d}} \quad \text{valid for } \min(\sigma_{22}) \geq 0 \tag{25}$$

where $CGR^d$ is the crack growth rate for a particular damage mode at the maximum ERR loading and $\varphi_0^d$ and $n^d$ are fitting parameters for the Paris' Law relationships. It should be noted that the normalisation in (26) has only been validated for $R_s^d > 0$ and the normalisation in (27) has only been validated to work for situations where crack faces remain stress free during the entire loading cycle, i.e. $\sigma_{22,min} \geq 0$. The stochastic nature of both crack initiation and crack growth are modelled using the Weibull distributions. This result in two SN fields for initiation where the SN fields for the initiation damage modes are given as:

$$P_f^d\left(N_{fat}^d, \sigma_{\max}^d, \sigma_{\min}^d\right) = 1 - exp\left(-\left[\frac{N_{fat}^d}{\left(\frac{\psi^d}{\psi_0^d}\right)^{\frac{1}{m^d}}}\right]^{\beta_s^d}\right) \quad \text{for d = LHS, LMPS} \tag{26}$$

where $\beta_s^d$ is the Weibull shape parameters. In the same way for off-axis crack propagation the crack growth fields are given as:

$$P_c^d\left(CGR^d, G_{\max}^d, G_{\min}^d\right) = 1 - exp\left(-\left[\frac{CGR^d}{\varphi_0^d(\varphi^d)^{n^d}}\right]^{\beta_c^d}\right) \tag{27}$$

where $\beta_c^d$ is the Weibull shape parameters for the LHS and LMPS propagation damage modes. Eq. (26)-(27) which describe the influence of LHS related damage modes on the fatigue evolution along with the similar equation for the LMPS damage modes essentially contain the full set of material parameters included in the model. The full set of material parameters can be obtained from uni-axial quasi-static and fatigue tests on two different MD laminates.

A simplified parameterisation of the crack evolution process was proposed in order to establish a computational efficient model based on the LHS equations (26)-(27) along with the similar equations for the LMPS damage modes. Figure 26 illustrates a RVE with initiation elements used to assess when cracks will initiate and crack elements in which off-axis cracks may grow.

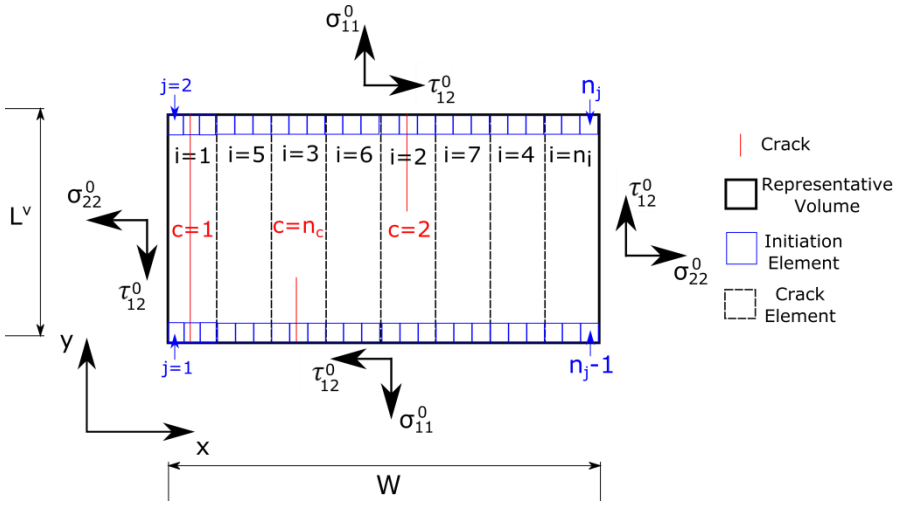


*Figure 26: Schematic of the modelled crack evolution process along with the used notation.*

The numbers of the crack elements express the order in which the cracks initiate. Furthermore, they are similar to the crack doubling concept, where cracks are assumed to initiate in the middle between already existing cracks. This location experiences the highest stress and consequently the risk of off-axis crack initiation is highest here. Furthermore, the parameterisation assumes that off-axis cracks grow across the full specimen width. This parametrisation was chosen, because this allowed for establishing the location and stress intensity factor for each crack a-priori to the fatigue simulation. This simplifies the required computational effort as

the location does not need to be stored, and the stress intensity factors do not need to be evaluated for each simulated cycle step.

The model should be evaluated through an iterative scheme and the flowchart for simulation of an MD laminate is given in Figure 27.

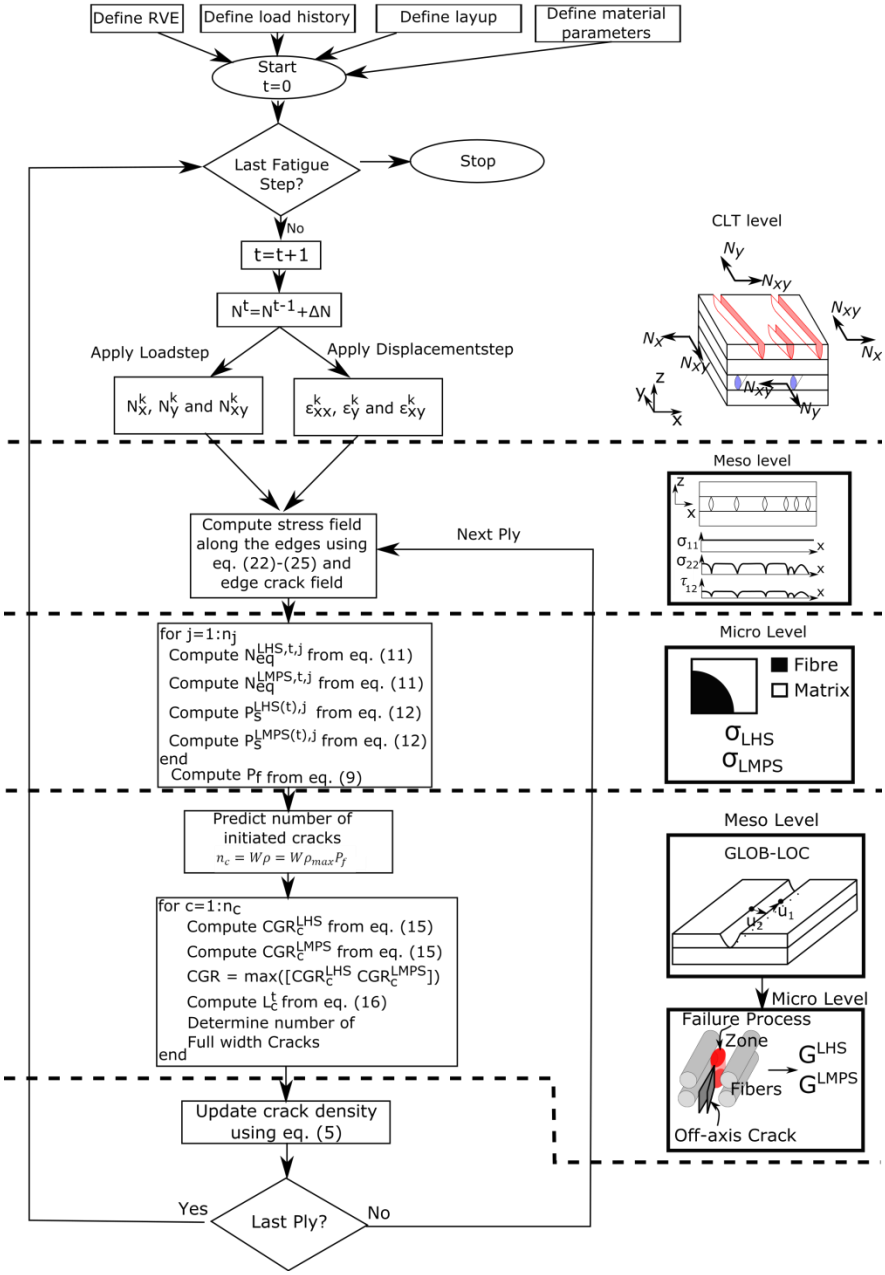


*Figure 27: Flowchart for the crack density calculation. Equation numbers refer to equations in Paper #4.*

## 6.2. RESULTS

Two different MD laminates were tested in order to obtain evolution parameters for the LHS and LMPS damage modes. The obtained parameters are given in Table 3 in (Paper#4). Using the determined parameters it was tested whether the model was capable of predicting crack density evolution for another multiaxial stress state than the ones from which the material parameters were determined. Further on, the models applicability in terms of modelling the influence for VA block loading and a change in stress ratio was also studied.

Comparison of model predictions with the measured crack density using ACC for the thick layer in the $[0/-60/0/60]_s$ laminate tested in (Paper #2) is shown in Figure 28.

It is seen that model predictions agree well with the measured crack density. Comparisons for the thin layer were not included, since the thin layer showed a different crack evolution process, where cracks would not grow through the entire width of the specimen. This violates the simplifying assumption used in the model and consequently results in less accurate predictions.

## 6.3. CONCLUSIONS

The development of a multiaxial fatigue model for off-axis crack evolution resulted in the following novel conclusions:

- State-of-the-art physical based multiaxial fatigue models have been combined into a multi-scale multiaxial fatigue model to predict off-axis crack density evolution.
- Material parameters to describe damage evolution for the LHS and LMPS damage mechanisms have been derived using two different MD laminates along with ACC.
- The model has been shown to predict crack density evolution well for CA, VA and C-T loading indicating that the modelling approach is successful at modelling the different damage mechanisms leading to off-axis crack propagation.
- In its current form, the model is only capable of predicting crack density evolution when cracks predominantly grow through the entire width of the specimens. This is due to the simplified parametrisation used and this parametrisation should therefore be improved in future versions, so more generally applicable predictions can be made.

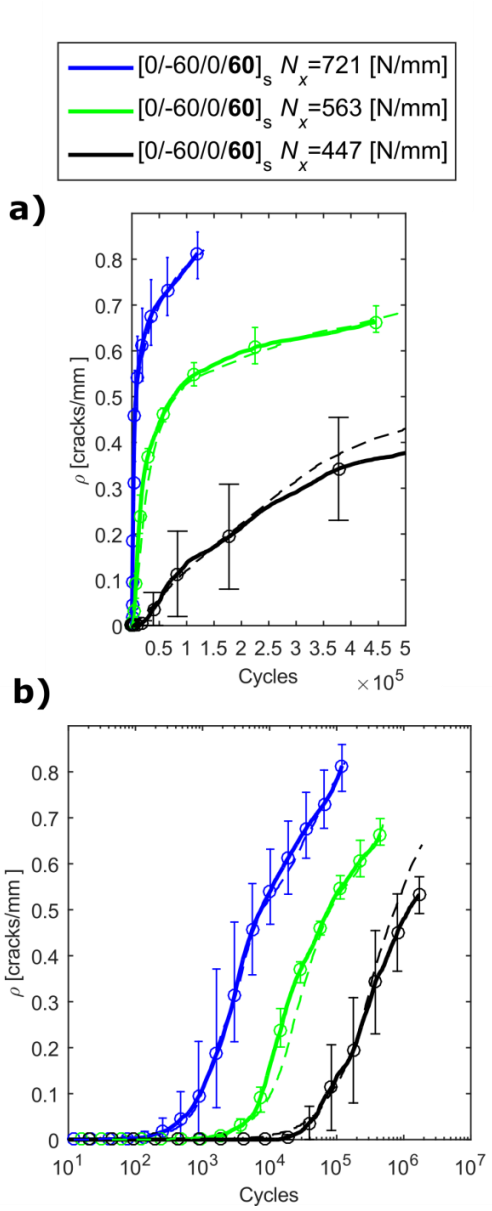


*Figure 28: Crack density results for the 60° layer in the [0/-60/0/60]s laminate tested in (Paper #2) subjected to CA fatigue loading at a load ratio of R=0.1. a) has a linear x axis scaling and b) has logarithmic x axis scaling. Solid lines represent experimentally measured crack density and dashed lines are model predictions (Paper #4).*

# CHAPTER 7. SUMMARY OF SCIENTIFIC CONTRIBUTIONS

In this chapter, this Ph.D.'s main contributions and novelty of the work carried out are highlighted. The contributions and novelty have been divided into knowledge produced and methods developed.

(Paper #1) describes the first-ever method to automatically quantify off-axis cracks in GFRP laminates. The method is called ACC, is non-destructive and eliminates the manually and visually counting of off-axis cracks, which represents a labour intensive and difficult task. The method therefore makes it possible to create better direct comparison between test series and analyse more tests than was possible before.

In the work of (Paper #2), ACC is combined with lock-in DIC and extensometer to establish a method capable of assessing the damage in-situ in MD GFRP laminates. This method is used to study the damage evolution in an MD laminate subjected to CA T-T, CA C-T and VA T-T loading. This study led to an increased knowledge about the damage evolution process as well as new methods to derive physically based evolution parameters defining the off-axis crack evolution process. The new knowledge included that crack density is a suitable damage measure for VA loading and that T-T loading results in a higher crack density evolution rate and apparent saturation value than C-T loading. Furthermore, the stochastic nature of off-axis crack initiation and growth is accurately modelled by the Weibull distribution and the shape-parameter of the Weibull distribution is constant for different stress levels. The Weibull shape parameter therefore represents a material property needed to model the off-axis crack evolution process. Additionally, new knowledge about the performance of the GLOB-LOC model was obtained, where it was found that the GLOB-LOC slightly under-predicts the stiffness of the degraded laminate but in general can be considered accurate when compared to phenomenological approaches like the sudden ply discount method.

(Paper #3) includes a reanalysis of observed and reported damage mechanisms where epoxy is used to bond stiff constituents together. It was found that the same two damage mechanisms have been observed and reported in numerous publications for different epoxy material systems. From this knowledge, a physically based model for mixed-mode crack propagation was proposed. The model predicts when each of the two damage mechanisms occur and how they influence crack propagation. The model is used to reanalyse crack growth data obtained from literature and it was found that the model was capable of collapsing crack growth data into one master curve for each of the two underlying damage mechanism. Furthermore, the transition between master curves was predicted by the model to

occur at the same mode-mixity, where images of fracture surfaces reveal a shift in damage mechanism. As the Ph.D. project focused on the modelling of off-axis cracks, the work in (Paper #3) also included a new multi-scale modelling approach to evaluate the physically mixed-mode crack propagation model in a computational efficient manner.

The main contribution of the work presented in (Paper #4) is focused on method development of a multi-scale multiaxial fatigue model for off-axis crack density evolution. The model is based on a physically based model for off-axis crack initiation obtained from literature, the mixed-mode propagation model from (Paper #3) and the GLOB-LOC modelling framework. The work also includes an extension of the GLOB-LOC model so additional information can be obtained from the model. The additional information includes the influence of off-axis crack interaction on the CSD and the ability to compute the varying stress field between off-axis cracks.

# CHAPTER 8. FUTURE WORK

As described in previous chapters, this Ph.D. project has solved problems in measuring, quantifying and modelling the off-axis crack evolution process for multiaxial fatigue loading. However, even though the present thesis establishes a methodology to characterise a given GFRP material and uses this characterisation in a modelling framework to predict the off-axis crack evolution, there still exist several topics within the field of off-axis crack evolution that need further research. The following list includes the main research gaps found at the completion of this Ph.D. project.

- Investigate whether the number of parameters needed in ACC can be reduced in order to ease the use of the algorithm and study how changes in the experimental setup (lighting conditions, camera alignment, specimen thickness/transparency, resin, roving, fabric and stitching types etc.) influence the counting.
- In the study and determination of evolution parameters only isolated cracks were considered. However, with the increased temporal resolution of the crack evolution provided by ACC it would be interesting to study the successive generation of non-isolated off-axis cracks. Such a study could potentially provide further insight in how damage accumulates for VA loading and which damage accumulation laws are applicable at the micro-scale.
- Both the initiation model used and the crack propagation model developed in this research use a phenomenological approach to take into account the load-ratio influence. For most composite structures (including wind turbine blades), the load ratio does not remain constant during service. It is thus clear, that there is a great need to gain further insight into how the load-ratio influence the off-axis crack evolution and how to model it.
- Since off-axis crack evolution is a hierarchical process involving several different length scales, additional research is needed to clarify the influence of the geometry of the test specimen/structure on the crack evolution process in order to mature the methods for structural scale analysis.
- It would be of great interest to composite manufactures to have models capable of predicting ultimate structural failure, which is a feature not included in the current model. Ultimate structural failure usually occurs as a result of fibre failure in the laminate layers. The model proposed in this Ph.D. project provides information on the load increase in the fibres when off-axis cracks are present. It is not clear whether this information along with SN-curves for fibre failure is sufficient to create accurate predictions for fibre failure or if the off-axis crack evolution alters the damage process in the fibres such that the fibre failure SN-curves no longer are applicable.

Additional research in clarifying the interaction between off-axis cracks and fibre failure is therefore an important future research topic.

# LITERATURE LIST

[1] The European GRP market in 2016. Reinf Plast 2017;61:73–4. doi:10.1016/j.repl.2017.01.026.

[2] Soden P., Kaddour A., Hinton M. Recommendations for designers and researchers resulting from the world-wide failure exercise. Compos Sci Technol 2004;64:589–604. doi:10.1016/S0266-3538(03)00228-8.

[3] Broņdsted P, Nijssen RPL. Advances in wind turbine blade design and materials. Woodhead Publishing; 2013.

[4] DNV-GL. DNVGL-ST-0376: Rotor blades for wind turbines. 2015.

[5] BSI. BS EN 61400-1 Wind Turbines - Design Requirements. 2005.

[6] Germanischer Lloyd. Guideline for the certification of wind turbines. 2003.

[7] Stevens RL, Fatemi A, Stephens RR, Fuchs HO. Metal fatigue in engineering. 2nd ed. John Wiley & Sons, Inc; 2001.

[8] Schijve J. Fatigue of Structures and Materials. Secaucus, NJ, USA: Kluwer Academic Publishers; 2001.

[9] Jamison, Russell D. Characterization and analysis of damage mechanisms in tension-tension fatigue of graphite/epoxy laminates. vol. 1. ASTM International; 1984.

[10] Quaresimin M, Susmel L, Talreja R. Fatigue behaviour and life assessment of composite laminates under multiaxial loadings. Int J Fatigue 2010;32:2–16. doi:10.1016/j.ijfatigue.2009.02.012.

[11] Degrieck J, Van Paepegem W. Fatigue damage modeling of fibre-reinforced composite materials: Review. Appl Mech Rev 2001;54:279. doi:10.1115/1.1381395.

[12] Quaresimin M. 50 th anniversary article: multiaxial fatigue testing of composites: from the pioneers to future directions. Strain 2015;51:16–29. doi:10.1111/str.12124.

[13] Talreja R. Multi-scale modeling in damage mechanics of composite materials. J Mater Sci 2006;41:6800–12. doi:10.1007/s10853-006-0210-9.

[14] Lundmark P, Varna J. Constitutive relationships for laminates with ply cracks in in-plane loading. Int J Damage Mech 2005;14:235–59. doi:10.1177/1056789505050355.

[15] Wharmby A. Observations on damage development in fibre reinforced polymer laminates under cyclic loading. Int J Fatigue 2003;25:437–46. doi:10.1016/s0142-1123(02)00118-4.

[16] Zangenberg J, Brondsted P, Gillespie JW. Fatigue damage propagation in unidirectional glass fibre reinforced composites made of a non-crimp fabric. J Compos Mater 2013;48:2711–27. doi:10.1177/0021998313502062.

[17] Tong J, Guild FJ, Ogin SL, Smith PA. Off-axis fatigue crack growth and the associated energy release rate in composite laminates. Appl Compos Mater 1997;4:349–59. doi:10.1007/BF02481399.

[18] Wharmby AW, Ellyin F. Damage growth in constrained angle-ply laminates under cyclic loading. Compos Sci Technol 2002;62:1239–47. doi:10.1016/s0266-3538(02)00075-1.

[19] Adden S, Horst P. Stiffness degradation under fatigue in multiaxially loaded non-crimped-fabrics. Int J Fatigue 2010;32:108–22. doi:10.1016/j.ijfatigue.2009.02.002.

[20] Quaresimin M, Carraro PA, Mikkelsen LP, Lucato N, Vivian L, Brøndsted P, et al. Damage evolution under cyclic multiaxial stress state: A comparative analysis between glass/epoxy laminates and tubes. Compos Part B Eng 2014;61:282–90. doi:10.1016/j.compositesb.2014.01.056.

[21] Kaddour A, Hinton M, Smith P, Li S. The background to the third world-wide failure exercise. J Compos Mater 2013;47:2417–26. doi:10.1177/0021998313499475.

[22] Emery TR, Dulieu-Barton JM. Thermoelastic Stress Analysis of damage mechanisms in composite materials. Compos Part A Appl Sci Manuf 2010;41:1729–42. doi:10.1016/j.compositesa.2009.08.015.

[23] Battams G. The use of optical techniques to assess the damage tolerance of composite materials, PhD dissertation. phdthesis. University of Southampton, 2014.

[24] Li L, Lomov S V, Yan X, Carvelli V. Cluster analysis of acoustic emission signals for 2D and 3D woven glass/epoxy composites. Compos Struct 2014;116:286–99. doi:10.1016/j.compstruct.2014.05.023.

[25] Guild FJ, Vrellos N, Drinkwater BW, Balhi N, Ogin SL, Smith PA. Intra-laminar cracking in CFRP laminates: observations and modelling. J Mater Sci 2006;41:6599–609. doi:10.1007/s10853-006-0199-0.

[26] Sket F, Enfedaque A, Alton C, González C, Molina-Aldareguia JM, Llorca J. Automatic quantification of matrix cracking and fiber rotation by X-ray computed tomography in shear-deformed carbon fiber-reinforced laminates. Compos Sci Technol 2014;90:129–38. doi:10.1016/j.compscitech.2013.10.022.

[27] Sisodia S, Gamstedt EK, Edgren F, Varna J. Effects of voids on quasi-static and tension fatigue behaviour of carbon-fibre composite laminates. J Compos Mater 2015;49:2137–48. doi:10.1177/0021998314541993.

[28] Wolodko JD, Hoover JW, Ellyin F. Detection of transverse cracks in GFRP composites using digital image processing. In: Ellyin F, Provan JW, editors. Prog. Mech. Behav. Mater. (ICM8), vol 2 Mater. Prop., University of Victoria, Departement of Mechanical Engineering; 1999, p. 483–7.

[29] Glud JA, Dulieu-Barton JM, Thomsen OT, Overgaard LCT. Automated counting of off-axis tunnelling cracks using digital image processing. Compos Sci Technol 2016;125:80–9. doi:10.1016/j.compscitech.2016.01.019.

[30] Daugman JG. Uncertainty relation for resolution in space, spatial frequency, and orientation optimized by two-dimensional visual cortical filters. JOSA A 1985;2:1160–9.

[31] Otsu N. A threshold selection method from gray-level histograms. IEEE Trans Syst Man Cybern 1979;9:62–6.

[32] Lam L, Lee SW, Suen C. Thinning methodologies: a comprehensive survey. IEEE Trans Pattern Anal Mach Intell 1992;14:869–85.

[33] Nijssen R. Optidat - database reference document. Kluisgat 5 1771 MV Wieringerwerf, the Netherlands: 2006.

[34] Mandell JF, Samborsky D. DOE / MSU composite material fatigue database. 2009.

[35] Jones RM. Mechanics of Composite Materials. 2nd ed. Taylor & Francis Group; 1999.

[36] Shokrieh MM, Lessard LB. Progressive fatigue damage modeling of composite materials, Part I: Modeling. J Compos Mater 2000;34:1056–80. doi:10.1177/002199830003401301.

[37] Eliopoulos EN, Philippidis TP. A progressive damage simulation algorithm for GFRP composites under cyclic loading. Part I: Material constitutive model. Compos Sci Technol 2011;71:742–9. doi:10.1016/j.compscitech.2011.01.023.

[38] Kennedy CR, Brádaigh CMÓ, Leen SB. A multiaxial fatigue damage model for fibre reinforced polymer composites. Compos Struct 2013;106:201–10. doi:10.1016/j.compstruct.2013.05.024.

[39] Passipoularidis VA, Philippidis TP, Brondsted P. Fatigue life prediction in composites using progressive damage modelling under block and spectrum loading. Int J Fatigue 2011;33:132–44. doi:10.1016/j.ijfatigue.2010.07.011.

[40] Tong J, Guild FJ, Ogin SL, Smith PA. On matrix crack growth in quasi-isotropic laminates - I. Experimental investigation. Compos Sci Technol 1997;57:1527–35. doi:10.1016/s0266-3538(97)00080-8.

[41] Adden S, Horst P. Damage propagation in non-crimp fabrics under bi-axial static and fatigue loading. Compos Sci Technol 2006;66:626–33. doi:10.1016/j.compscitech.2005.07.034.

[42] Li C, Ellyin F, Wharmby A. On matrix crack saturation in composite laminates. Compos Part B Eng 2003;34:473–80. doi:10.1016/S1359-8368(03)00020-9.

[43] Fruehmann RK, Dulieu-Barton JM, Quinn S, Tyler JP. The use of a lock-in amplifier to apply digital image correlation to cyclically loaded components. Opt Lasers Eng 2015;68:149–59. doi:10.1016/j.optlaseng.2014.12.021.

[44] Reifsnider KL. Damage in composite materials: basic mechanisms, accumulation, tolerance, and characterization. ASTM; 1982. doi:10.1520/STP775-EB.

[45] Quaresimin M, Carraro PA, Maragoni L. Influence of load ratio on the biaxial fatigue behaviour and damage evolution in glass/epoxy tubes under tension–torsion loading. Compos Part A Appl Sci Manuf 2015;78:294–302. doi:10.1016/j.compositesa.2015.08.009.

[46] Boniface L, Ogin SL. Application of the paris equation to the fatigue growth of transverse ply cracks. J Compos Mater 1989;23:735–54. doi:10.1177/002199838902300706.

[47] Singh C V, Talreja R. A synergistic damage mechanics approach for composite laminates with matrix cracks in multiple orientations. Mech Mater 2009;41:954–68. doi:10.1016/j.mechmat.2009.02.008.

[48] Carraro PA, Quaresimin M. A stiffness degradation model for cracked multidirectional laminates with cracks in multiple layers. Int J Solids Struct 2015;58:34–51. doi:10.1016/j.ijsolstr.2014.12.016.

[49] Nairn JA, Mendels DA. On the use of planar shear-lag methods for stress-transfer analysis of multilayered composites. Mech Mater 2001;33:335–62. doi:10.1016/S0167-6636(01)00056-4.

[50] Hashin Z. Analysis of cracked laminates: a variational approach. Mech Mater 1985;4:121–36. doi:10.1016/0167-6636(85)90011-0.

[51] Lundmark P, Varna J. Crack face sliding effect on stiffness of laminates with ply cracks. Compos Sci Technol 2006;66:1444–54. doi:10.1016/j.compscitech.2005.08.016.

[52] Lundmark P, Varna J. Stiffness reduction in laminates at high intralaminar crack density: effect of crack interaction n.d. doi:10.1177/1056789509351840.

[53] Varna J. Modelling mechanical performance of damaged laminates. J Compos Mater 2013;47:2443–74. doi:10.1177/0021998312469241.

[54] Quaresimin M, Carraro PA, Maragoni L. Early stage damage in off-axis plies under fatigue loading. Compos Sci Technol 2016;128:147–54. doi:10.1016/j.compscitech.2016.03.015.

[55] Varna J, Krasnikovs A, Kumar RS, Talreja R. A synergistic damage mechanics approach to viscoelastic response of cracked cross-ply laminates. Int J Damage Mech 2004;13:301–34. doi:10.1177/1056789504042457.

[56] Nairn JA, Hu S, Bark JS. A critical evaluation of theories for predicting microcracking in composite laminates. J Mater Sci 1993;28:5099–111. doi:10.1007/BF00361186.

[57] Carraro PA, Quaresimin M. A damage based model for crack initiation in unidirectional composites under multiaxial cyclic loading. Compos Sci Technol 2014;99:154–63. doi:10.1016/j.compscitech.2014.05.012.

[58] Quaresimin M, Carraro PA. Damage initiation and evolution in glass/epoxy tubes subjected to combined tension-torsion fatigue loading. Int J Fatigue 2014;63:25–35. doi:10.1016/j.ijfatigue.2014.01.002.

[59] Carraro PA, Meneghetti G, Quaresimin M, Ricotta M. Crack propagation analysis in composite bonded joints under mixed-mode (I+II) static and fatigue loading: experimental investigation and phenomenological modelling. J Adhes Sci Technol 2013;27:1179–96. doi:10.1080/01694243.2012.735902.

[60] Bürger D, Rans CD, Benedictus R. Influence of fabric carrier on the fatigue disbond behavior of metal-to-metal bonded interfaces. J Adhes 2013.

[61] Armanios E, Bucinell R, Wilson D, Asp L, Sjögren A, Greenhalgh E. Delamination growth and thresholds in a carbon/epoxy composite under fatigue loading. J Compos Technol Res 2001;23:55. doi:10.1520/CTR10914J.

[62] Liu Z, Gibson RF, Newaz GM. The use of a modified mixed mode bending test for characterization of mixed-mode fracture behavior of adhesively bonded metal joints. J Adhes 2010;78:223–44. doi:10.1080/00218460210408.

[63] Purslow D. Matrix fractography of fibre-reinforced epoxy composites. Composites 1986;17:289–303. doi:10.1016/0010-4361(86)90746-9.

[64] Tanaka H, Tanaka K, Tsuji T, Katoh H. Mixed-mode (I+II) propagation of delamination fatigue cracks in unidirectional graphite/epoxy laminates. Trans Japan Soc Mech Eng Ser A 1999;65:1676–83. doi:10.1299/kikaia.65.1676.

[65] Kenane M, Benzeggagh ML. Mixed-mode delamination fracture toughness of unidirectional glass/epoxy composites under fatigue loading. Compos Sci Technol 1997;57:597–605. doi:10.1016/S0266-3538(97)00021-3.

[66] Bürger D. Mixed-mode fatigue disbond on metallic bonded joints, PhD dissertation. Delft University of Technology, 2015.

[67] Kawai M, Suda H. Effects of Non-Negative Mean Stress on the Off-Axis Fatigue Behavior of Unidirectional Carbon/Epoxy Composites at Room Temperature. J Compos Mater 2004;38:833–54. doi:10.1177/0021998304042477.

[68] Carraro PA. Multiaxial fatigue behaviour of composite materials: characterisation and modelling. PhD dissertation. University of Padova, 2014.

[69] Sun Z, Daniel IM, Luo JJ. Modeling of fatigue damage in a polymer matrix composite. Mater Sci Eng A 2003;361:302–11. doi:10.1016/S0921-5093(03)00556-2.

[70] Huang Y. Stochastic damage evolution under static and fatigue loading in composites with manufacturing defects. PhD dissertation. Texas A&M University, 2012.

[71] Kahla H Ben, Varna J, Pupurs A. Microcracking in layers of composite laminates in cyclic loading with tensile transverse stress component in layers. 20th Int. Conf. Compos. Mater., 2015.

# Appendix A. (Paper #1)

# Appendix B.  (Paper #2)

# Appendix C. (Paper #3)

# Appendix D. (Paper #4)

ISSN (online): 2446-1636
ISBN (online): 978-87-7112-961-8

AALBORG UNIVERSITY PRESS